Leyendo la borra del café ...

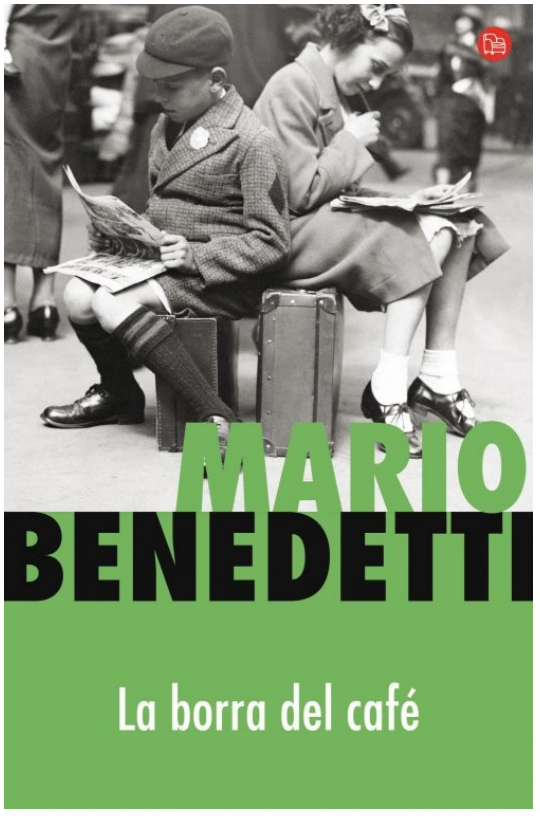
Leyendo la borra del café...

Desambiguacion wikipedica

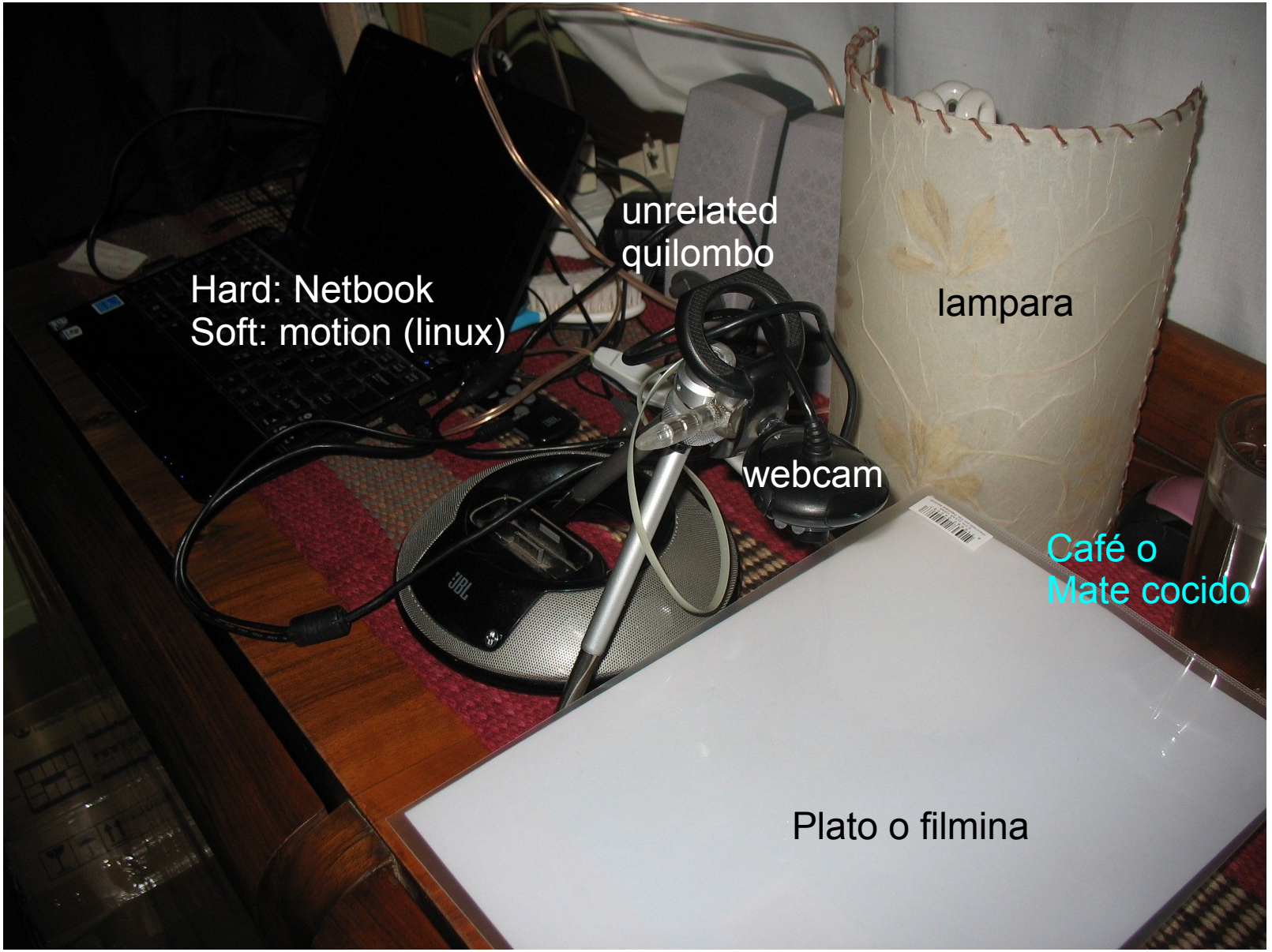
(1) Me refiero a leer esto:

"La borra del café, es el residuo que deja el café en la taza y que es interpretada por una persona especializada en el tema. Este hábito es una tradición originaria del medio oriente y consiste en interpretar, partiendo de la borra del café de una persona, su pasado, presente y futuro."

(2) No a leer la novela:



Experimental Setup

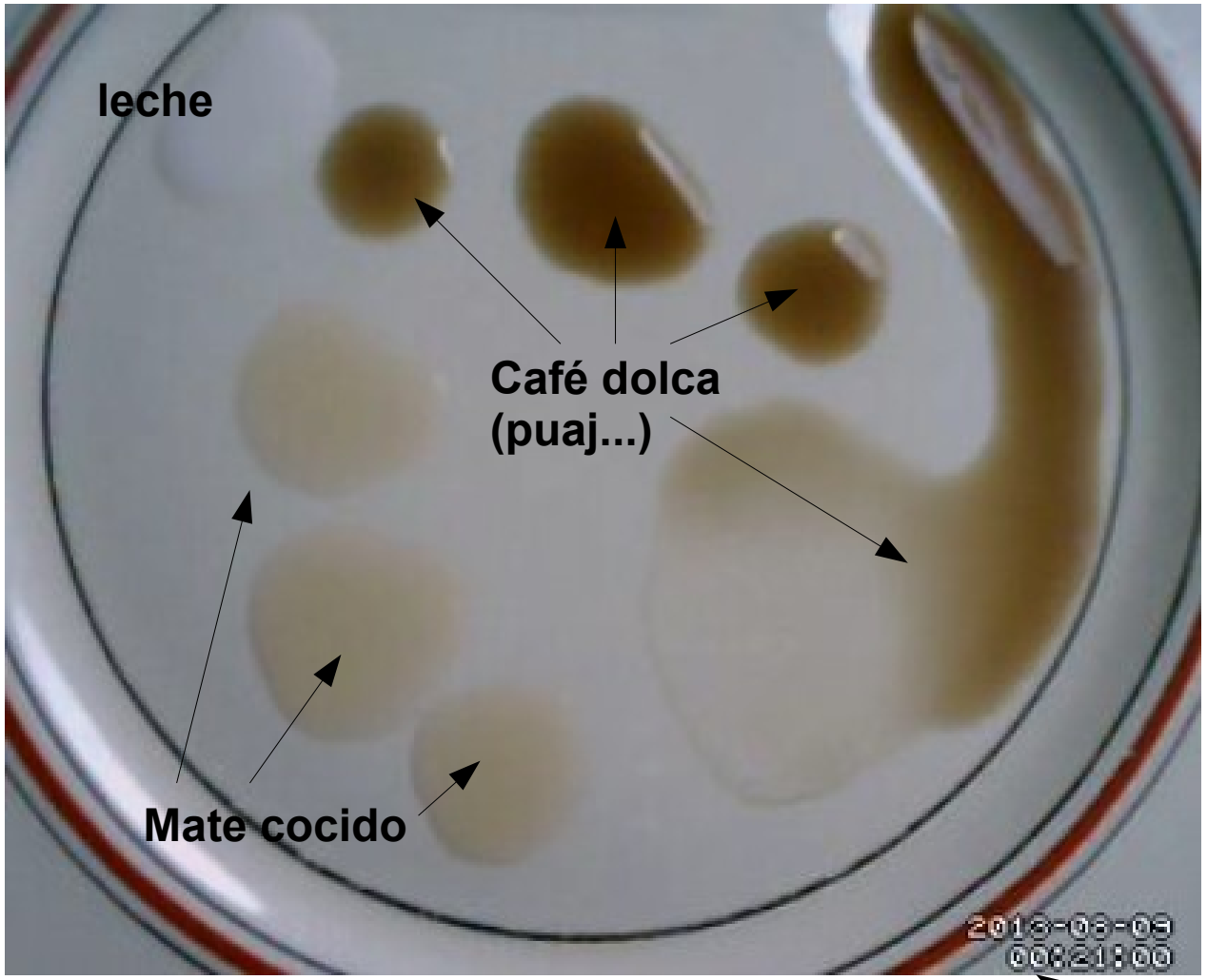


1 frame/ 30 seg
Por varias horas...

Los Coihues lab

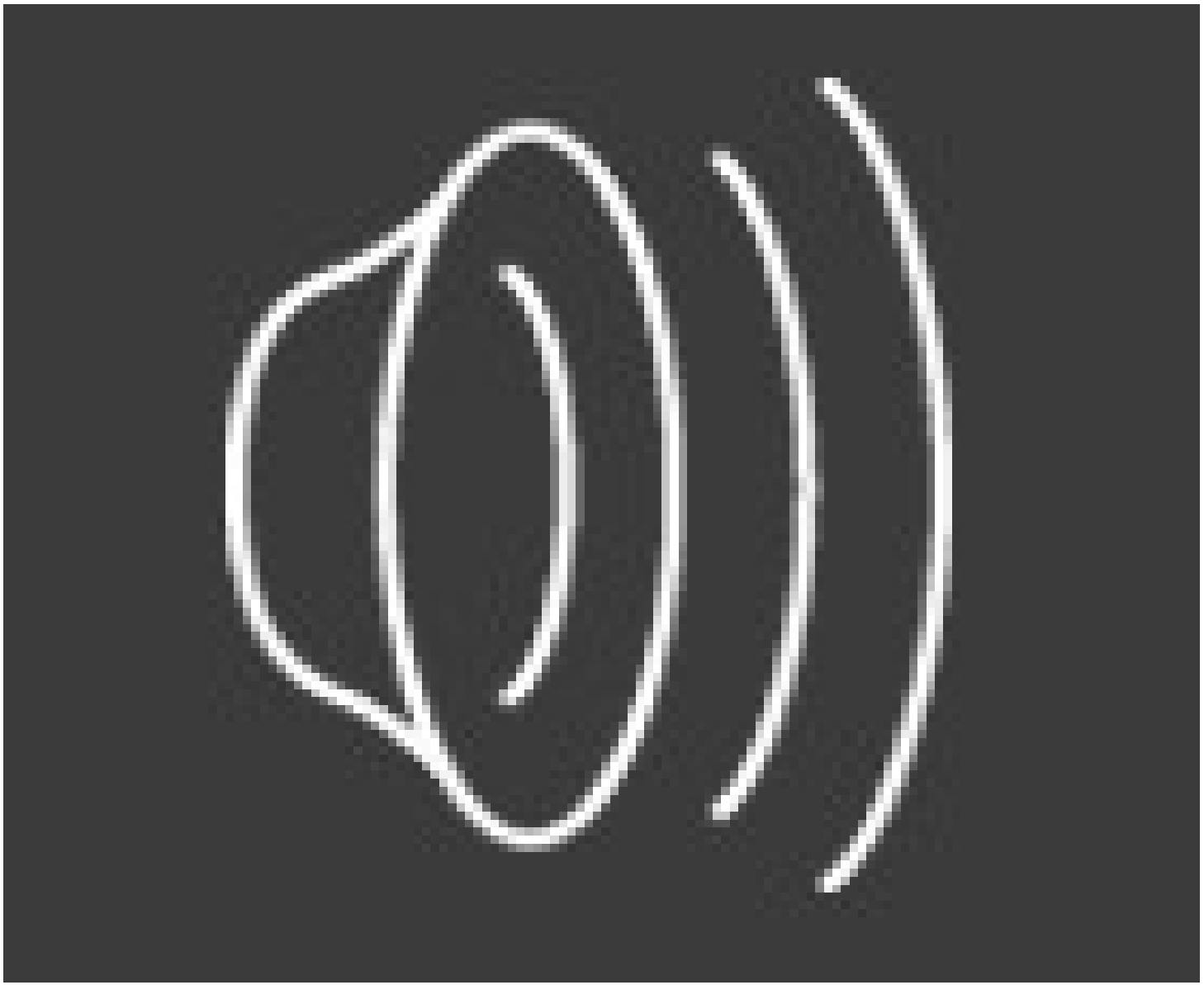
Evaporando gotas (de noche)

CONDICION INICIAL

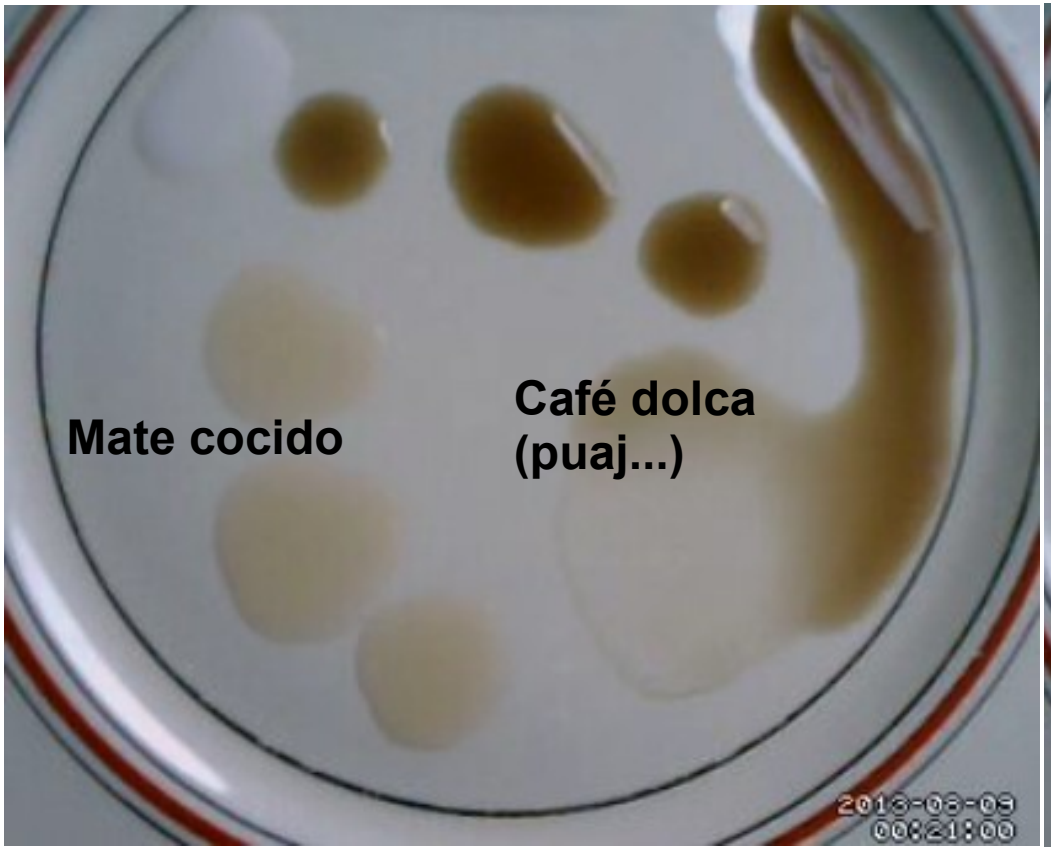


(h:m:s) Todos durmiendo...

Evaporando gotas (de noche)



Evaporando gotas (de noche)





ANTES

DESPUES

Fenómeno supercotidiano



Buscarlas en el fondo de la taza, o cerca de la maquina de café en la mesada, las mas interesantes en el piso....

Effects of Particle Shape on Growth Dynamics at Edges of Evaporating Drops of Colloidal Suspensions

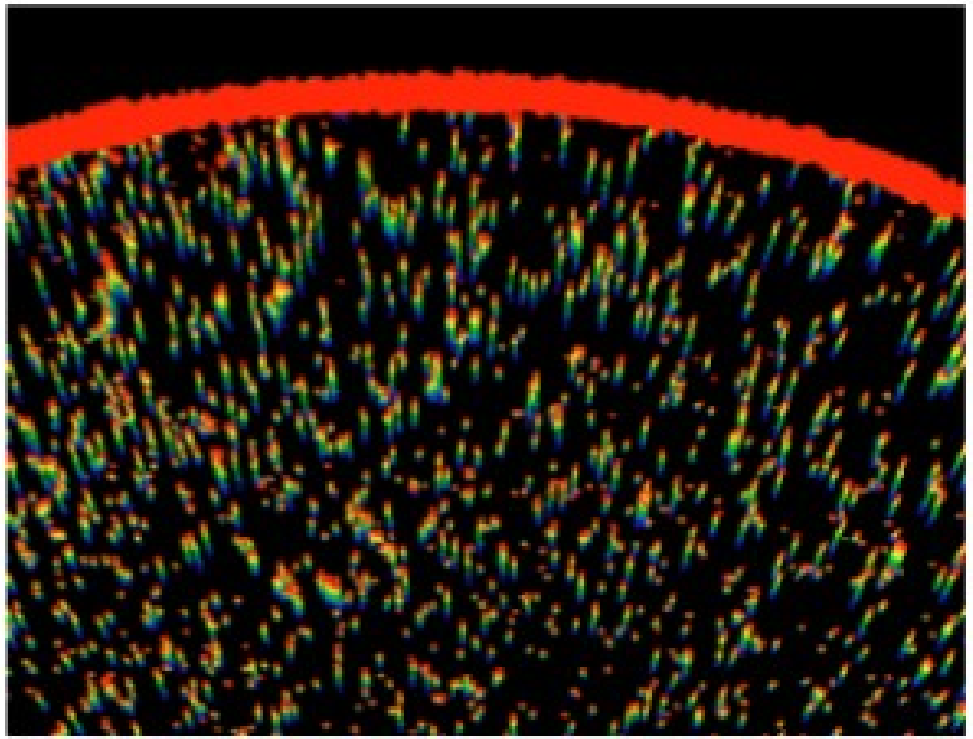
Peter J. Yunker,[1] Matthew A. Lohr,[1] Tim Still,[1,2] Alexei Borodin,[3] D. J. Durian,[1] and A. G. Yodh[1]

[1]*Department of Physics and Astronomy, University of Pennsylvania, Philadelphia, Pennsylvania 19104, USA*

[2]*Complex Assemblies of Soft Matter, CNRS-Rhodia-University of Pennsylvania, UMI 3254, Bristol, Pennsylvania 19007, USA*

[3]*Department of Mathematics, Massachusetts Institute of Technology, Cambridge, Massachusetts 02139, USA*

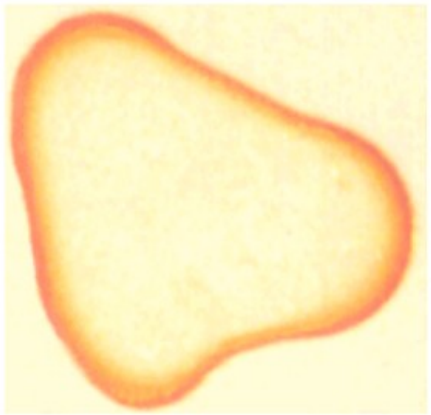
(Received 23 July 2012; published 18 January 2013)



Problema de deposicion,
o “surface growth”

Por que se forman?

NATURE | VOL 389 | 23 OCTOBER 1997



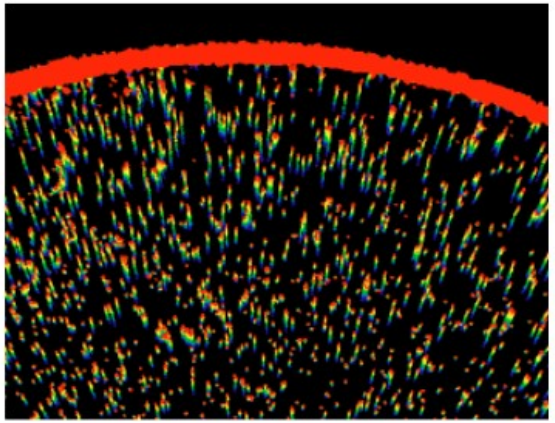


FIG. 1. a) A 2-cm-diameter drop of coffee containing one-weight-percent solids has dried to form a perimeter ring, accentuated in regions of high curvature. b) Video micrographs showing dispersion of fluorescent one-micron polystyrene spheres in water during evaporation, as described in the text. Multiple exposure shows different times in different colors to indicate the motion. Earliest time (blue) is 3 sec before latest time (red).

Capillary flow as the cause of ring stains from dried liquid drops

Robert D. Deegan*, Olgica Bakajin*, Todd F. Dupont†, Greb Huber*, Sidney R. Nagel* & Thomas A. Witten*

** James Franck Institute, 5640 South Ellis Avenue, Chicago, Illinois 60637, USA*
† Department of Computer Science, University of Chicago, 1100 East 58th Street, Chicago, Illinois 60637, USA

Our qualitative observations show that rings form for a wide variety of substrates, dispersed materials (solutes), and carrier liquids (solvents), as long as (1) the solvent meets the surface at a nonzero contact angle, (2) the contact line is pinned to its initial position, and (3) the solvent evaporates. In addition, we found that mechanisms typically responsible for solute transport—surface tension gradients, solute diffusion, electrostatic, and gravity effects—are negligible in ring formation. Based on these

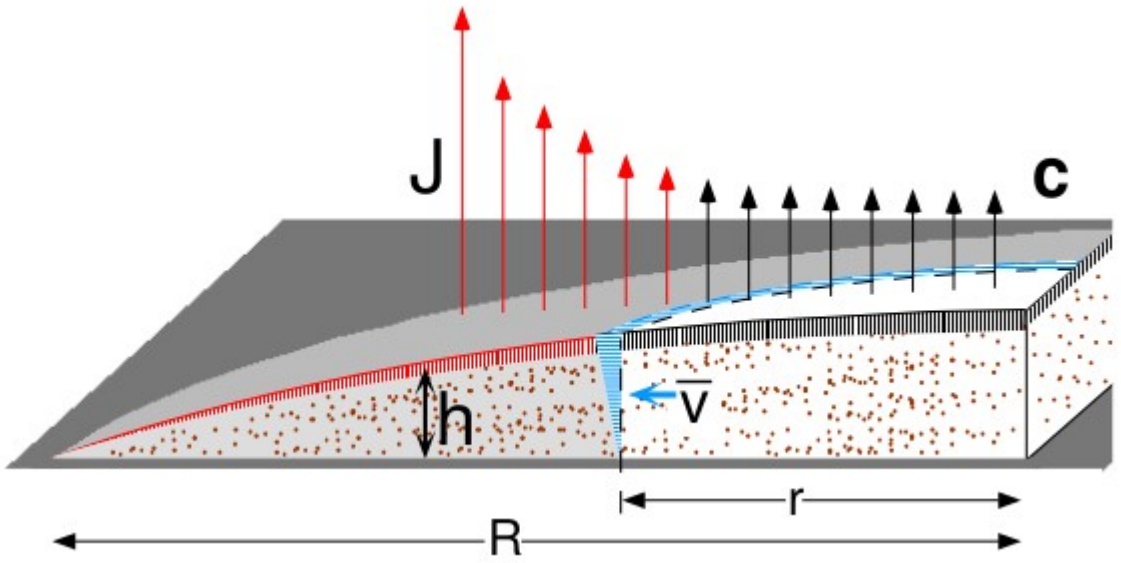
Por que se forman?

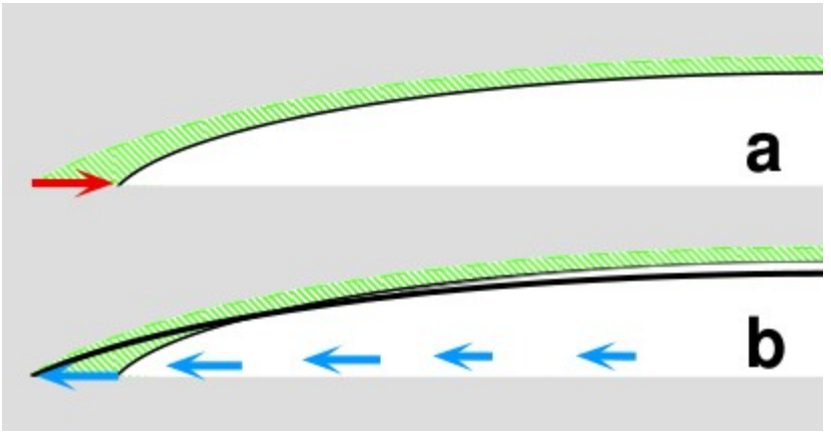
(1) Gotas: angulo de contacto, gravedad.

(2) Linea de contacto de mojado: anclaje.

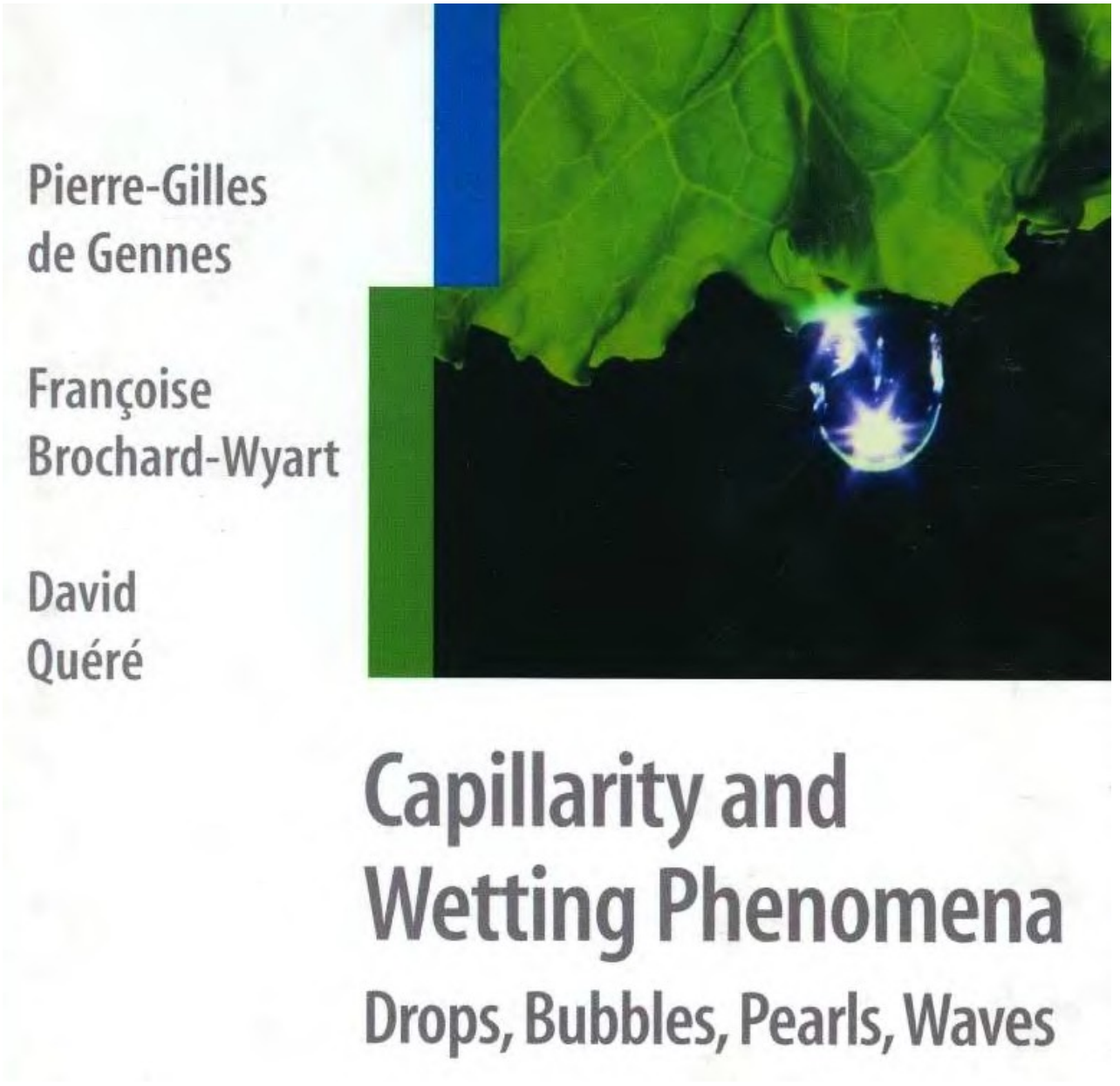
(3) Evaporación de la gota: no-uniforme.

(4) Flujo capilar: induce deposición convectiva del soluto en el borde de la gota.





Librazo


Pierre-Gilles
de Gennes
Françoise
Brochard-Wyart
David
Quéré
Capillarity and
Wetting Phenomena
Drops, Bubbles, Pearls, Waves

Wetting: Contacto entre tres fases

Spreading parameter

$$S = [E_{substrate}]_{dry} - [E_{substrate}]_{wet}$$

$$S = \gamma_{SO} - (\gamma_{SL} + \gamma),$$

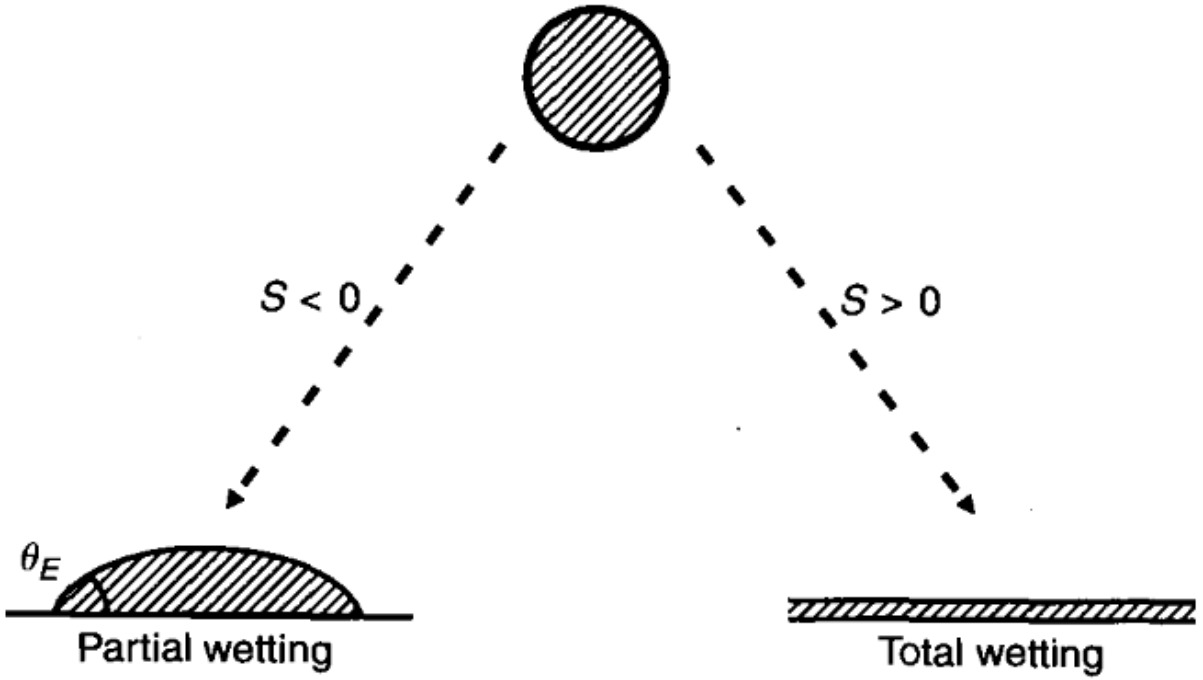


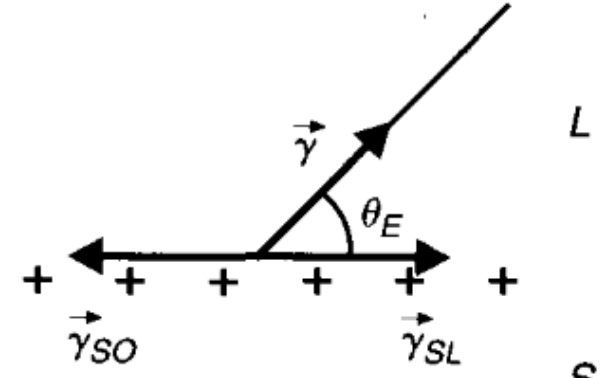
FIGURE 1.13. The two wetting regimes for sessile drops.

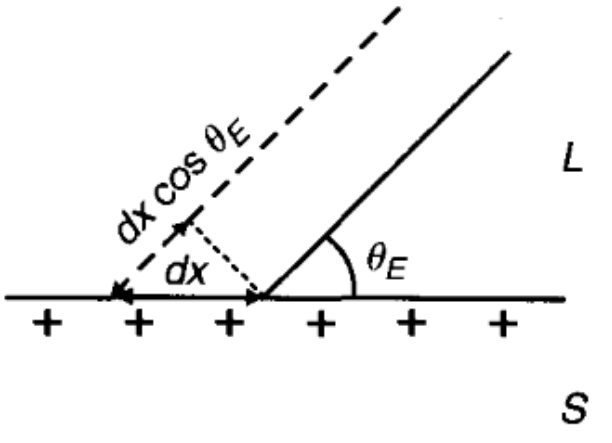
Contact Angle

Law of Young-Dupré

$$\gamma \cos\theta_E = \gamma_{SO} - \gamma_{SL}$$

$$S = \gamma(\cos\theta_E - 1)$$





Gotas

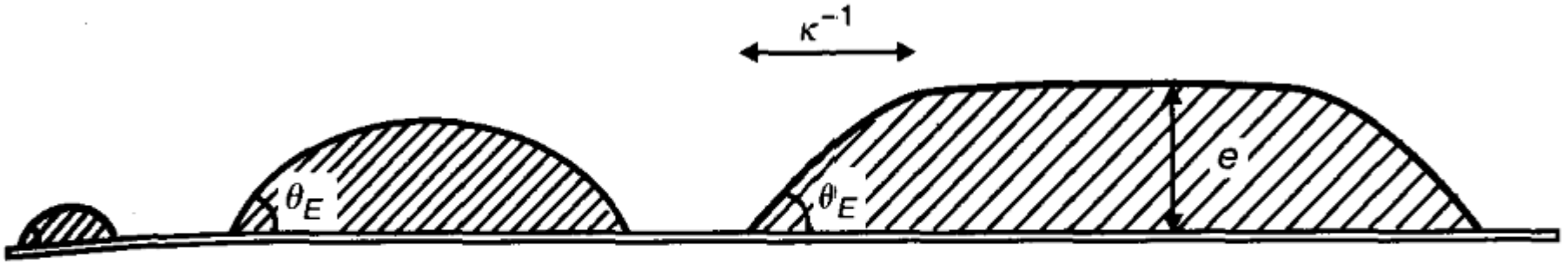


FIGURE 2.3. Water drops of increasing size on a sheet of plastic. Gravity causes the largest drops to flatten.

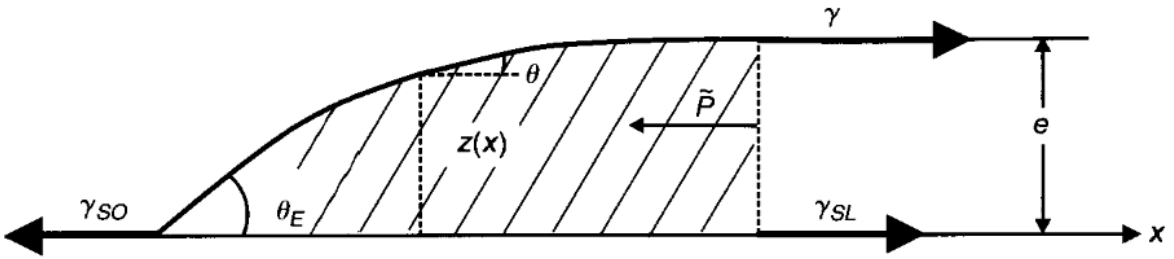
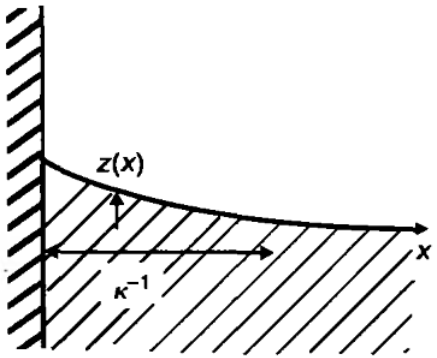


FIGURE 2.4. Equilibrium of the forces (per unit length of the line of contact) acting on the edge of a puddle. $\tilde{P} = \rho g e^2/2$ is the hydrostatic pressure.

Capillary length

$$\kappa^{-1} = \sqrt{\gamma/\rho g}$$



$$F_g = -SA + \frac{1}{2}\rho g e^2 A. \longrightarrow e = 2\kappa^{-1}\sin\left(\frac{\theta_E}{2}\right)$$

Gotas

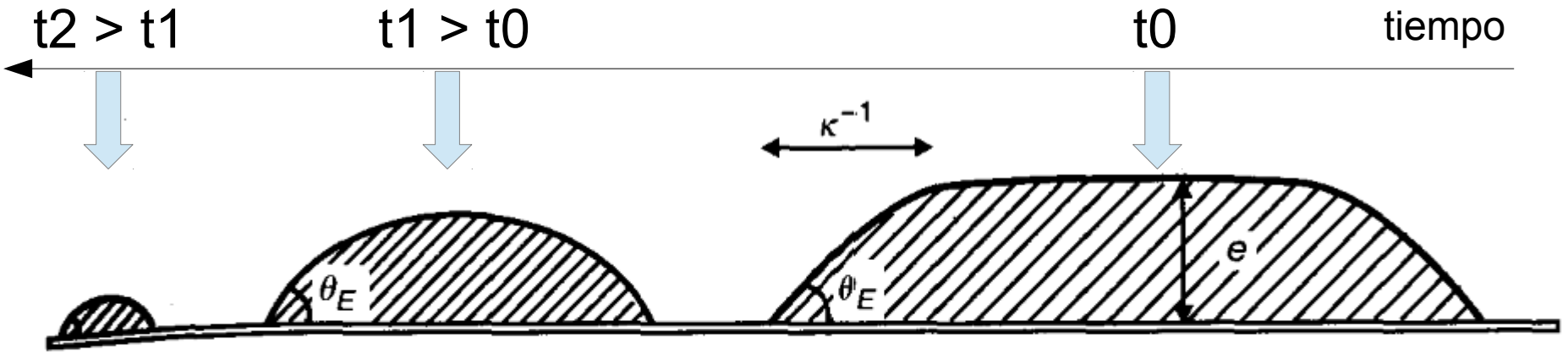


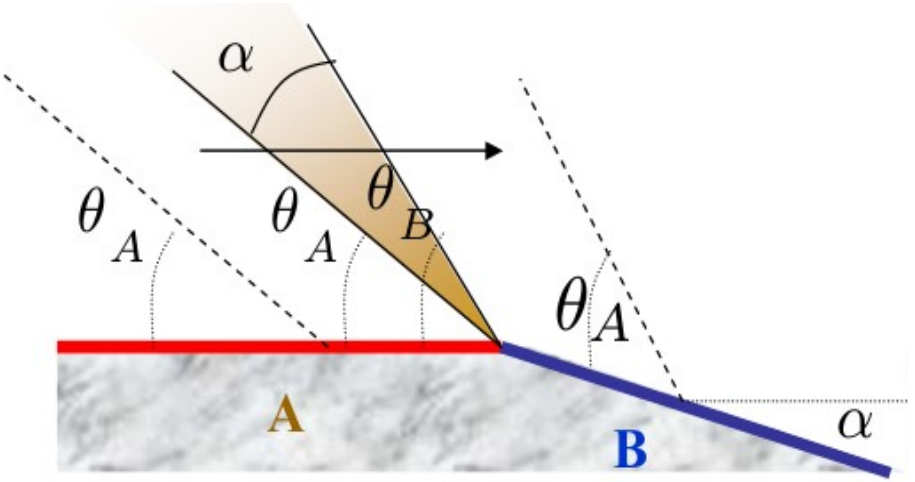
FIGURE 2.3. Water drops of increasing size on a sheet of plastic. Gravity causes the largest drops to flatten.

Porque no se evaporan así?

Efectos del desorden (localmente)

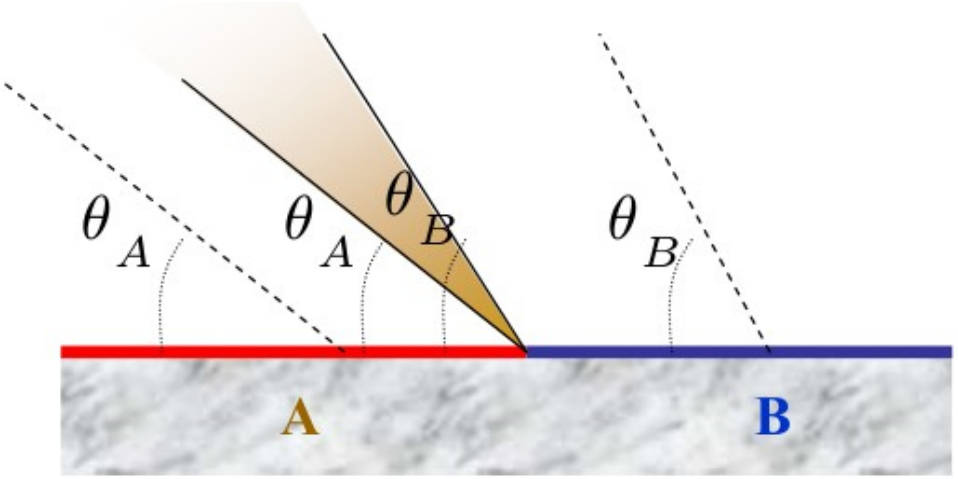
De Gennes, Rev. Mod. Phys. 1985

Pendientes locales (rugosidad)



$$F_p = \gamma\left(\cos(\theta+\alpha) - \cos\theta\right) \simeq -\gamma \sin\theta\alpha$$

Química heterogénea

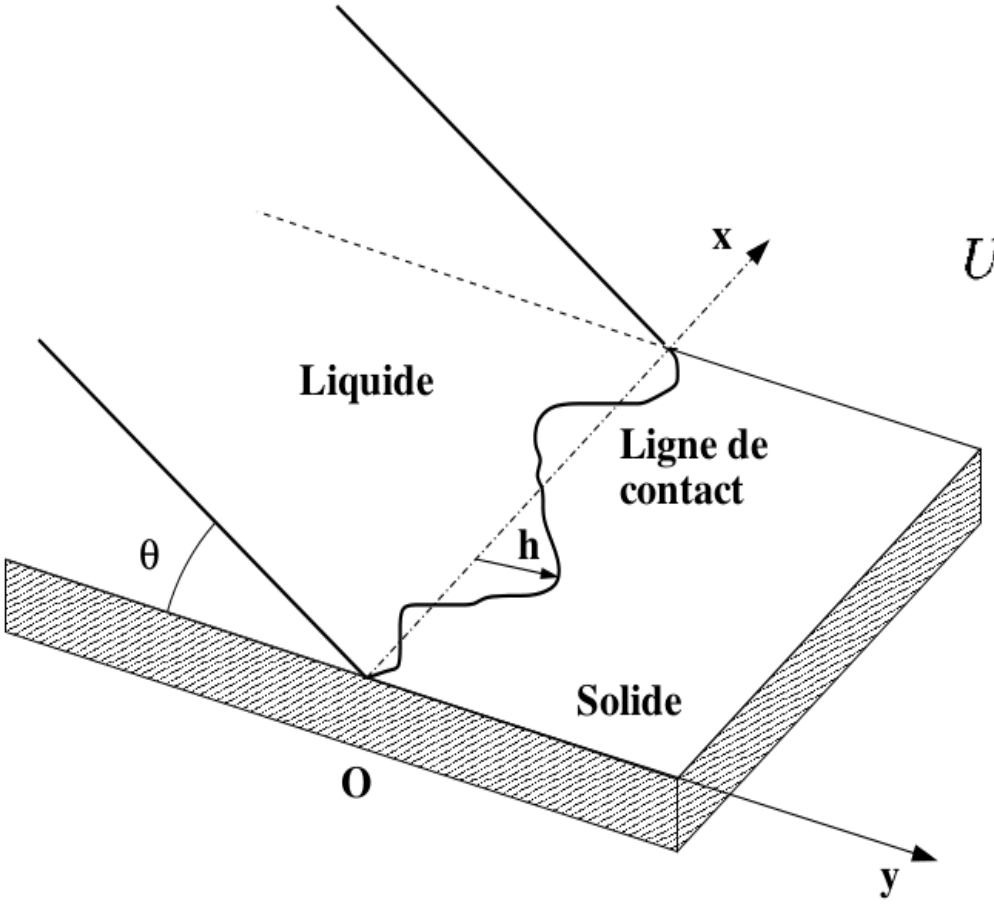


$$F_p = \gamma\left(\cos\theta_B - \cos\theta_A\right)$$

$$F_p = \gamma\left(\cos\left(\theta_B(x,t) + \alpha(x,t)\right) - \cos\theta_A\right)$$

Anclaje macroscópico de la linea de contacto: elasticidad vs desorden!

Elasticidad de la linea de contacto

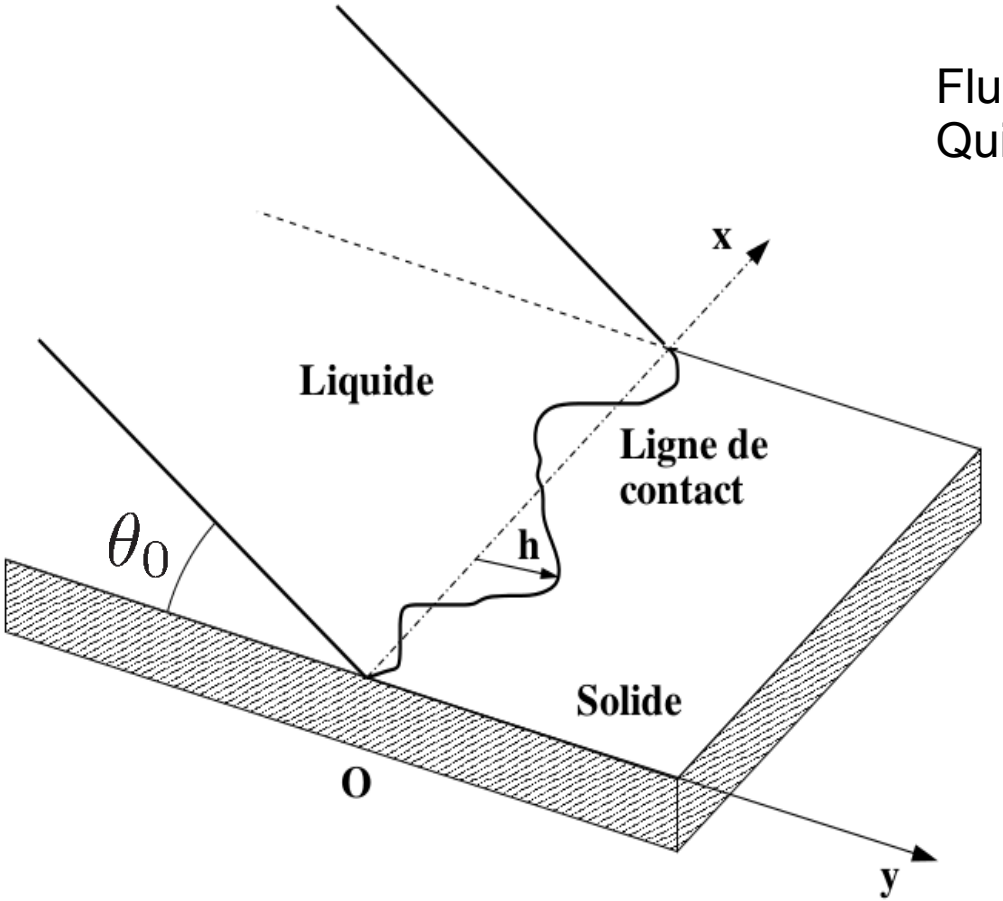


$$U_{\mathrm{cap}} = \frac{\gamma_{\mathrm{lg}}}{4}\sin^2(\theta)\int_{-\infty}^{+\infty}|k||\tilde{h}(k)|^2\frac{dk}{2\pi}.$$

Elasticidad de largo alcance

$$U_{\mathrm{cap}} = \frac{\gamma_{\mathrm{lg}}}{2\pi}\sin^2(\theta)\int_{a<|x-x'|<L}dxdx'\frac{(h(x')-h(x))^2}{(x-x')^2}.$$

Anclaje de la linea de contacto



Fluctuaciones espaciales en sustratos
Quimicamente heterogeneos o rugosos

Angulo de contacto no perturbado

$$\gamma \cos\theta_0 = \langle \gamma_{SV} - \gamma_{SL} \rangle$$

Fuerza de pinning local:

$$\eta(x,h) = \gamma(\cos(\theta) - \cos(\theta_0))$$

$$\frac{\partial}{\partial t} h(x,t) = f + \eta(x,h) - k \int dx_1 \frac{h(x,t) - h(x_1,t)}{(x - x_1)^2} .$$

Efectos del desorden

Histeresis
Del angulo
de contacto

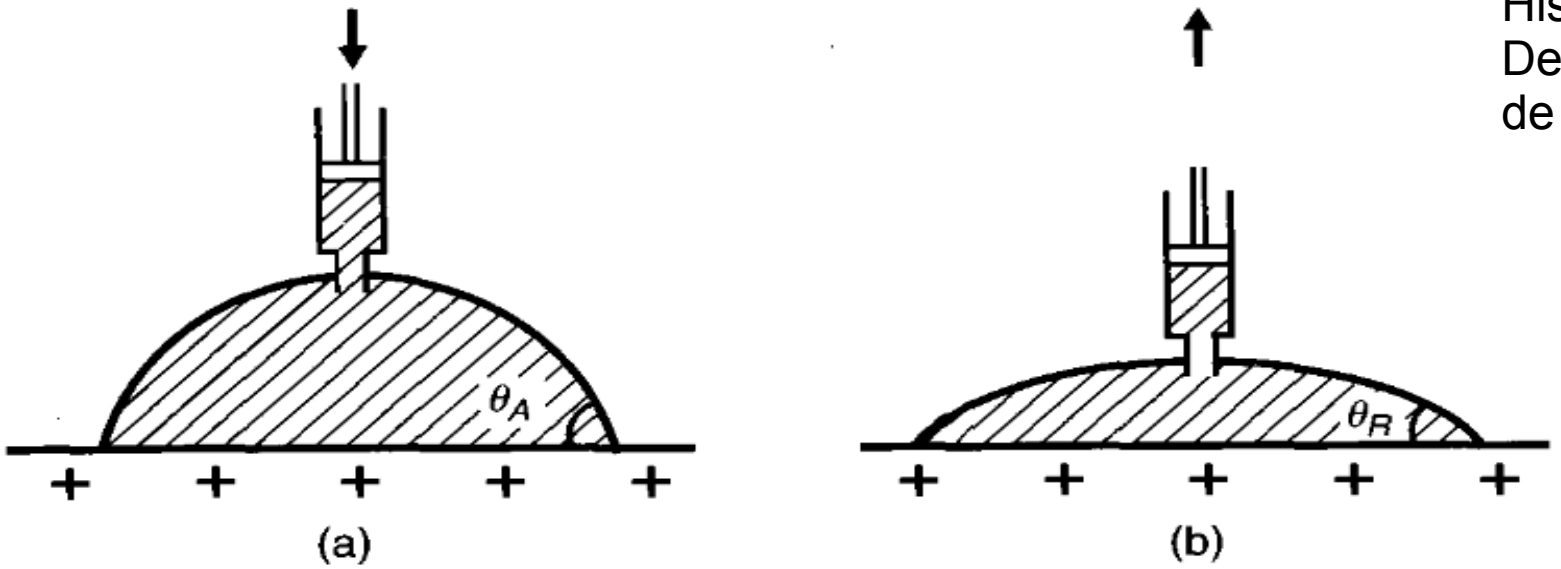
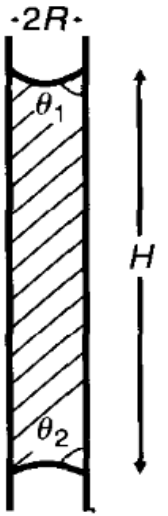


FIGURE 3.1. (a) Advancing angle when the drop is inflated; (b) receding angle when the drop is deflated.

Imposible en
Superficies
Perfectas!



$$\frac{2\gamma}{R}(\cos\theta_1 - \cos\theta_2) = \rho g H.$$

El equilibrio solo existe si:

$$\frac{2\gamma}{R}(\cos\theta_R - \cos\theta_A) > \rho g H.$$

Como se mide la fuerza de pinning

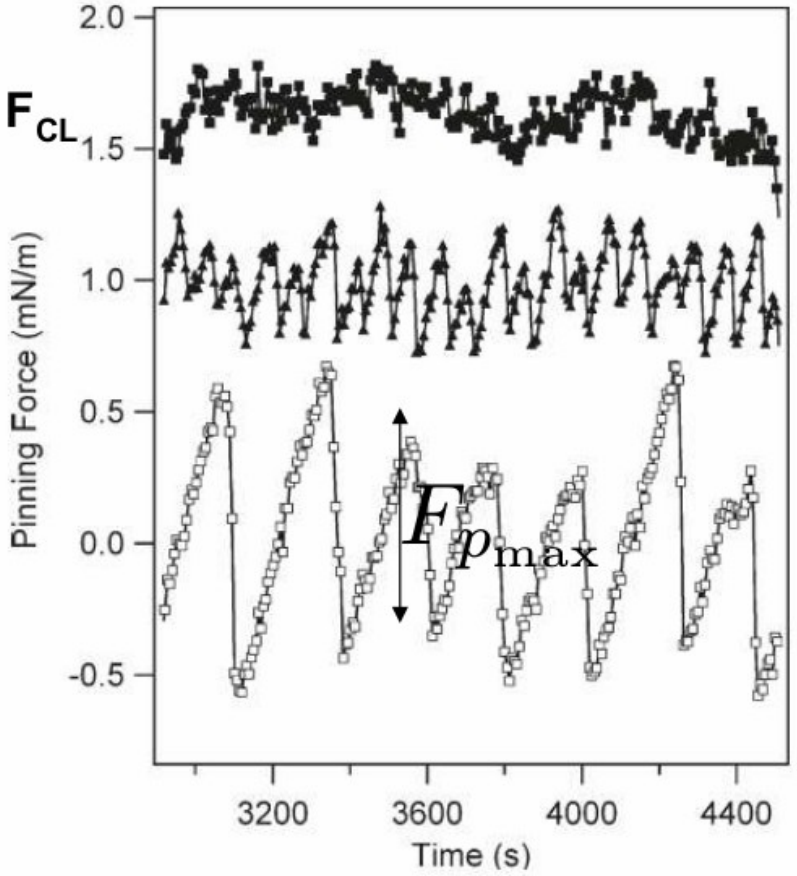
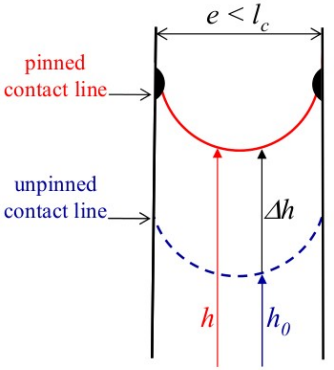


Figure 4. Examples of pinning force measurements. The data have been horizontally displaced for clarity. From the top to the bottom, the corresponding imposed velocities are 20, 9, and 3.5 μm s^{-1}. The weight fraction is 16%, temperature 25 °C, humidity 30%, and v_{evap} = 0.4 μm s^{-1}.

Pinning Force in capillary rise experiments



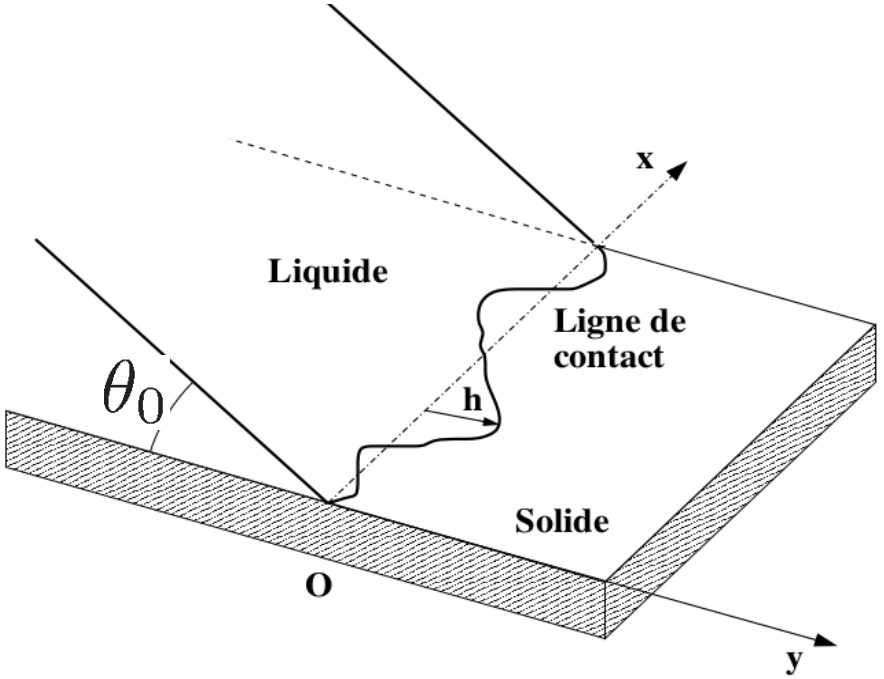
$$E(h) = -\gamma \cos\theta\, h + \frac{1}{2}\rho g e h^2$$

$$dE(h) = \left[-\gamma \cos\theta + \rho g e\, h\right] dh$$

Pinning force : $F_{CL} = \gamma\, \Delta(\cos\theta) = \rho g e\, \Delta h$

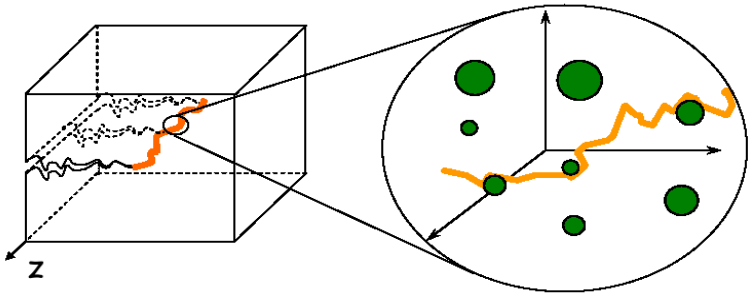
Dinámica de la línea de contacto

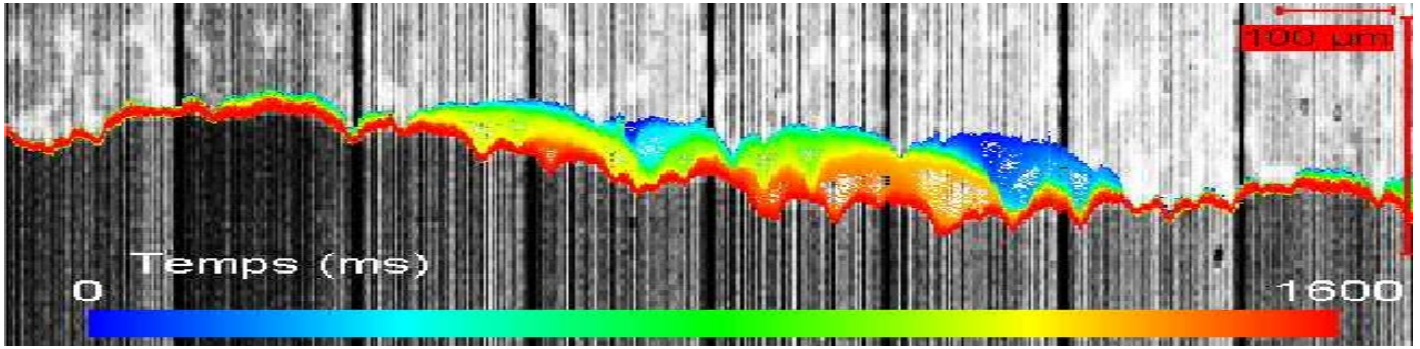
$$\frac{\partial}{\partial t}h(x,t) = f + \eta(x,h) - k\int dx_1 \frac{h(x,t) - h(x_1,t)}{(x-x_1)^2}\,.$$



Dinámica de interfaces en medios desordenados:

- Metastabilidad, Depinning, avalanchas, etc.
- Las fracturas tienen la misma elasticidad que la linea de contacto.





Dinámica de la línea de contacto

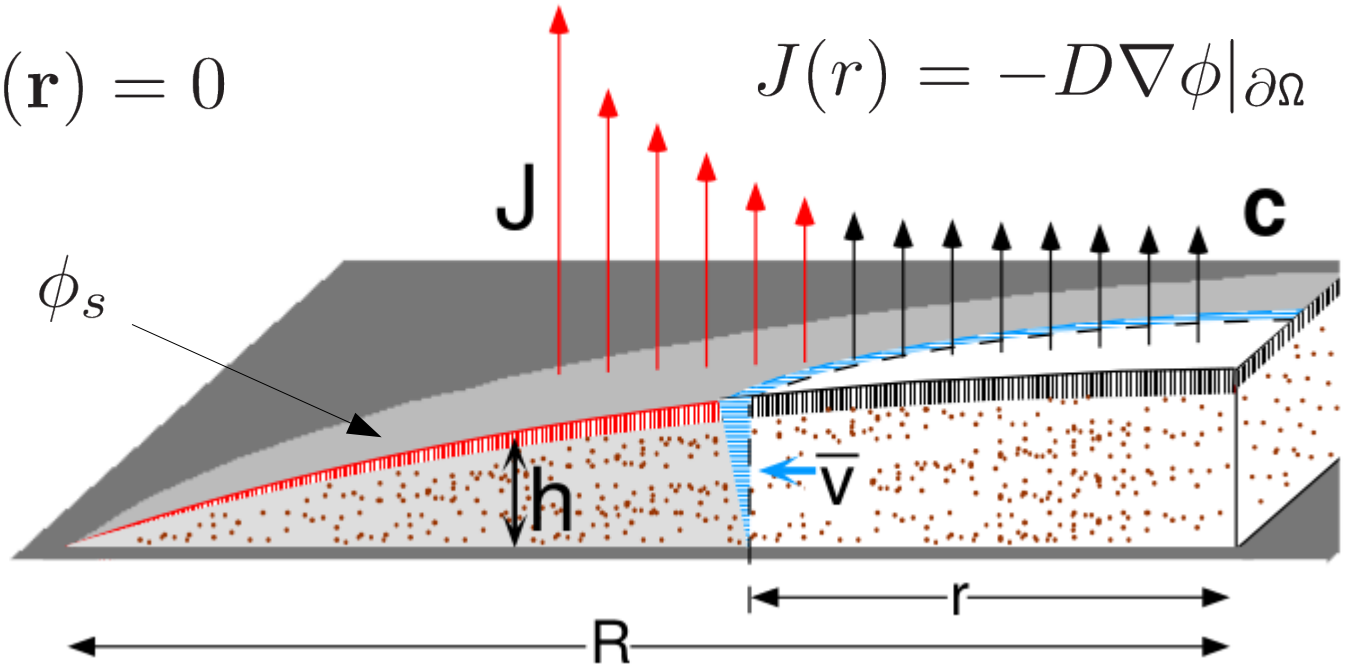
Lo muestro una vez mas?

ϕ_∞

Evaporación

$$\nabla^2\phi(\mathbf{r}) = 0$$

$$J(r) = -D\nabla\phi|_{\partial\Omega}$$

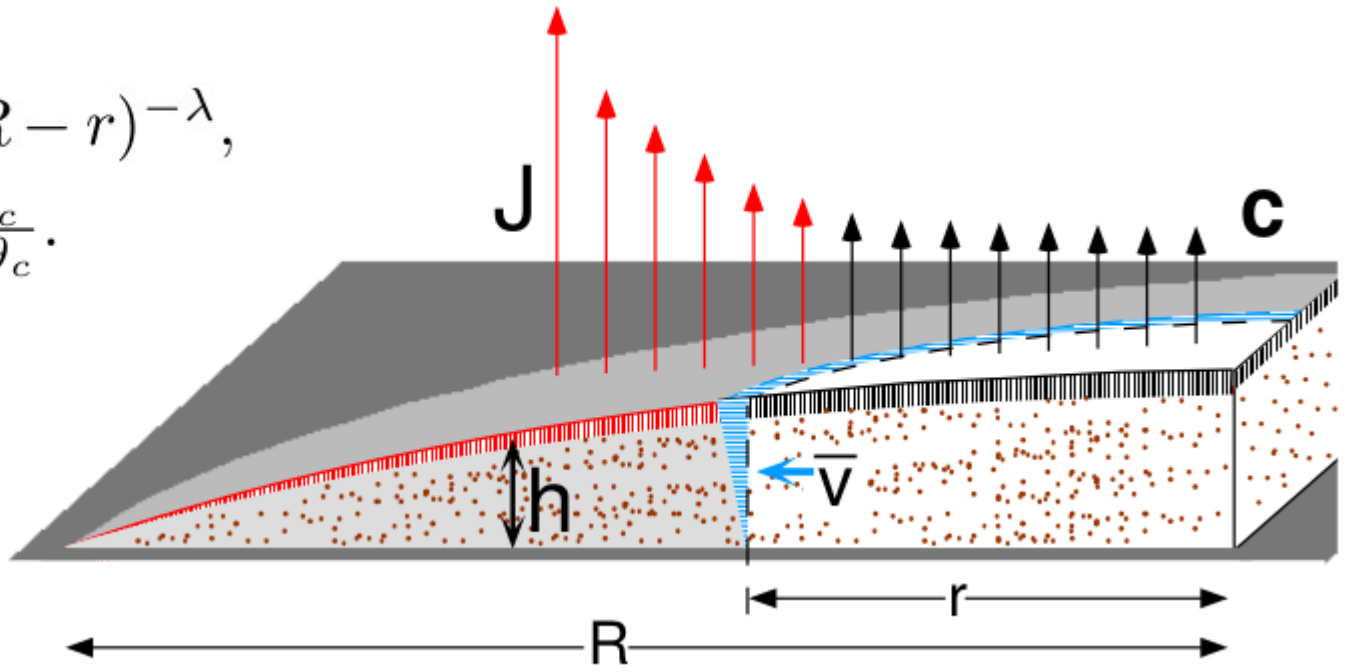


Problema de Electrostática

$$J(r) \sim (R-r)^{-\lambda}, \qquad \lambda = \frac{\pi - 2\theta_c}{2\pi - 2\theta_c}.$$

Transporte del soluto (inicial)

$$J(r) \sim (R-r)^{-\lambda},$$
$$\lambda = \frac{\pi - 2\theta_c}{2\pi - 2\theta_c}.$$



Evaporación no uniforme → Convección del fluido hacia el borde para compensar... $\bar{v} \sim J \sim (R-r)^{-\lambda}.$

Masa inicial a una distancia > r del centro $M(r,0) \sim (R-r)^2.$

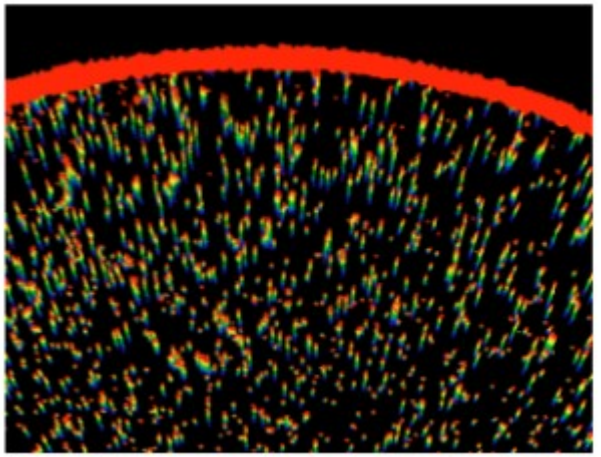
Tiempo para llegar al borde de una partícula en rt $$t = \int_{r_t}^{R} dr/\bar{v} \sim (R-r_t)^{1+\lambda},$$

Masa en el borde a tiempo t = la que tuvo el tiempo de llegar... $$M(R,t) = M(r_t,0) \sim t^{2/(1+\lambda)}.$$

Test experimental

$$M(R,t) = M(r_t, 0) \sim t^{2/(1+\lambda)}. \qquad \lambda = \frac{\pi - 2\theta_c}{2\pi - 2\theta_c}.$$

$$\theta_c \simeq .25 \text{ radians.} \Rightarrow 2/(1+\lambda) \approx 1.37$$



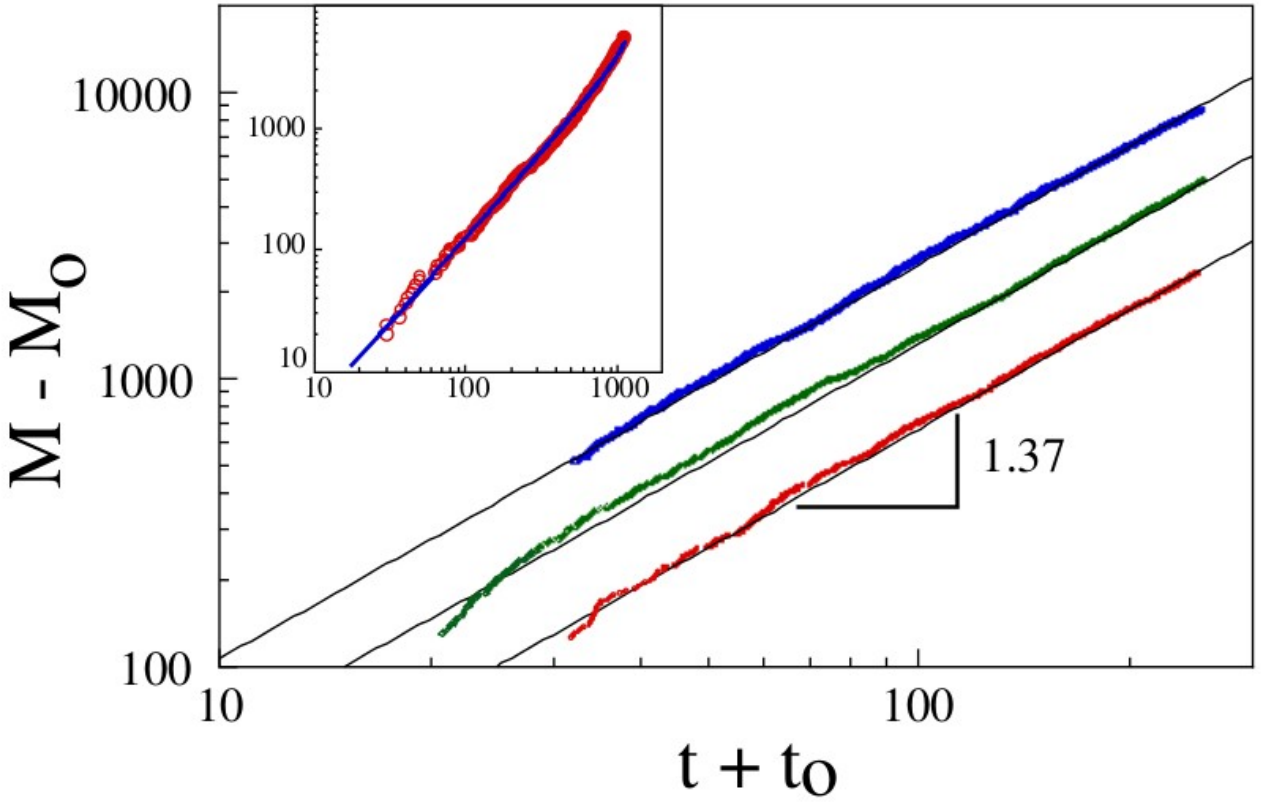


FIG 3. Double-logarithmic plot of ring mass $M(R,t)$ versus time t for times from 10 to 250 seconds after placement of the drop on the surface, for three different drops whose total drying time was about 800 sec. $M(R,t)$ is measured in number of particles. Particle number is counted in a sector of the ring similar to that shown in Figure 1b. An offset $M_0 = 2$ was subtracted from the lowest curve to account for early non-steady-state deposition. $M_0 = 50$ and 40 for the middle and upper curves. The upper curve coincided with the middle one and was shifted up by a factor of 2 for clarity. An offset $t_0 = 11$ sec, 13 sec and 10 sec was added to the time axis. The solid lines show the power law $(M - M_0) = \text{const}\ (t+t_0)^{1.37}$. Inset shows $M(R,t)$ versus t for the entire 1300-sec drying time. Circles: data obtained from ten-micron spheres via counting. Roughly 90 percent of the particles were observed to go to the contact line. Solid line: theoretical prediction determined numerically.

Supresión del anillo

- Condiciones:

Our qualitative observations show that rings form for a wide variety of substrates, dispersed materials (solutes), and carrier liquids (solvents), as long as (1) the solvent meets the surface at a nonzero contact angle, (2) the contact line is pinned to its initial position, and (3) the solvent evaporates. In addition, we found that mechanisms typically responsible for solute transport—surface tension gradients, solute diffusion, electrostatic, and gravity effects—are negligible in ring formation. Based on these

Supresión del anillo

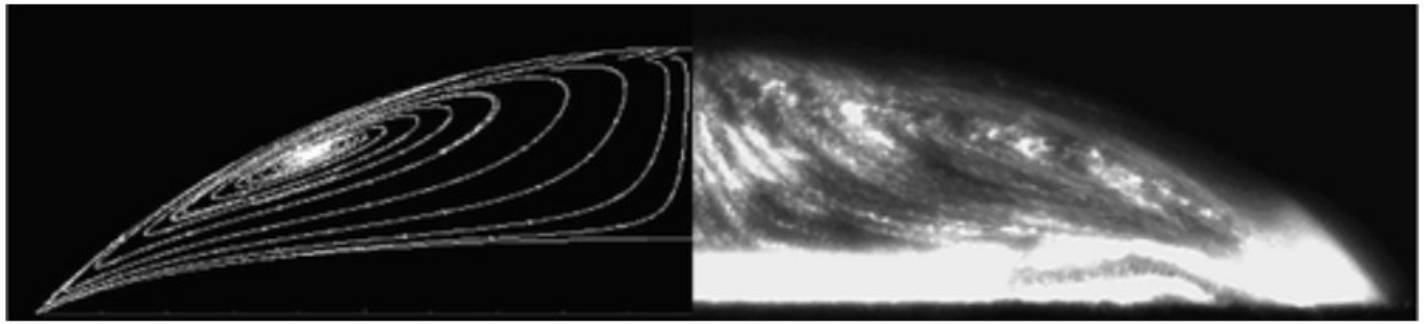
Marangoni Effect Reverses Coffee-Ring Depositions

THE JOURNAL OF PHYSICAL CHEMISTRY B LETTERS

Hua Hu*,† and Ronald G. Larson

Department of Chemical Engineering, University of Michigan, Ann Arbor, Michigan 48109-2136

Received: February 13, 2006; In Final Form: March 9, 2006



We show here both experimentally and theoretically that the formation of “coffee-ring” deposits observed at the edge of drying water droplets requires not only a pinned contact line (Deegan et al. *Nature* **1997**, *389*, 827) but also suppression of Marangoni flow. For simple organic fluids, deposition actually occurs preferentially at the center of the droplet, due to a recirculatory flow driven by surface-tension gradients produced by the latent heat of evaporation. The manipulation of this Marangoni flow in a drying droplet should allow one in principle to control and redirect evaporation-driven deposition and assembly of colloids and other materials.

[1]Department of Physics and Astronomy, University of Pennsylvania, Philadelphia, Pennsylvania 19104, USA. [2]Complex Assemblies of Soft Matter, CNRS-Rhodia-University of Pennsylvania UMI 3254, Bristol, Pennsylvania 19007, USA.

308 | NATURE | VOL 476 | 18 AUGUST 2011

Suppression of the coffee-ring effect by shape-dependent capillary interactions

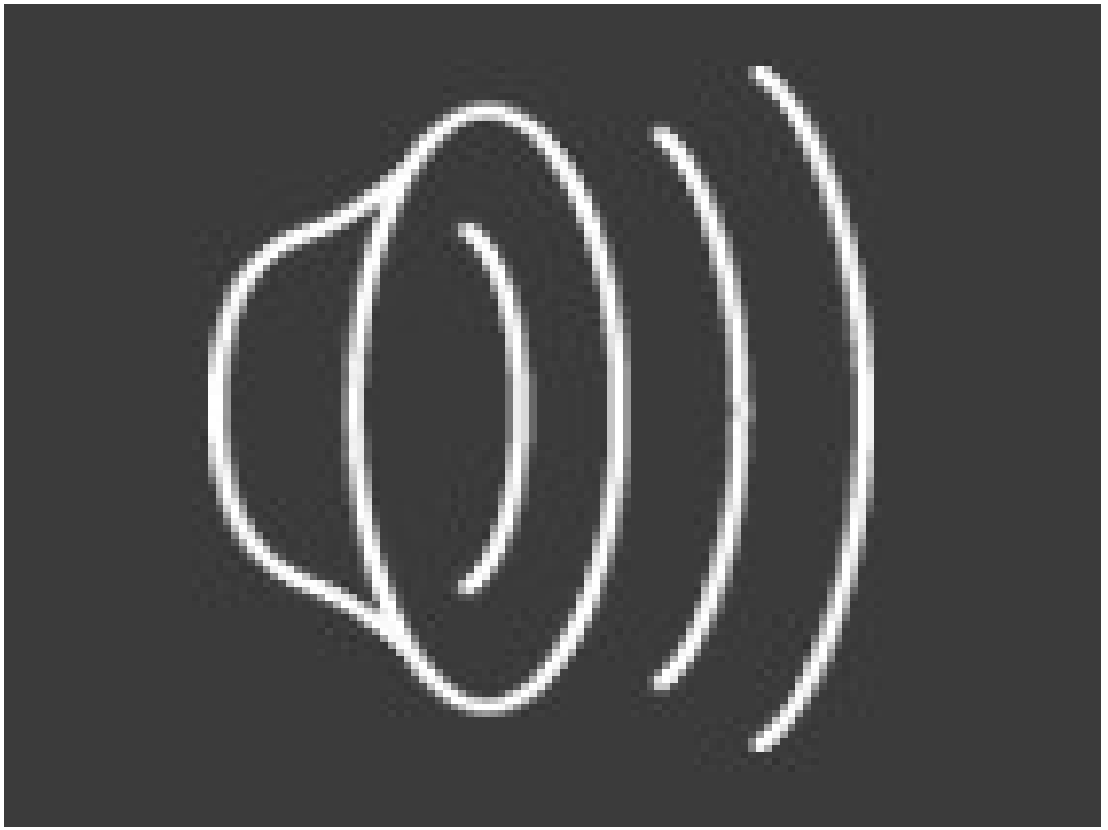
Peter J. Yunker[1], Tim Still[1,2], Matthew A. Lohr[1] & A. G. Yodh[1]

[1]Department of Physics and Astronomy, University of Pennsylvania, Philadelphia, Pennsylvania 19104, USA. [2]Complex Assemblies of Soft Matter, CNRS-Rhodia-University of Pennsylvania UMI 3254, Bristol, Pennsylvania 19007, USA.

308 | NATURE | VOL 476 | 18 AUGUST 2011

Suppression of the coffee-ring effect by shape-dependent capillary interactions

Peter J. Yunker[1], Tim Still[1,2], Matthew A. Lohr[1] & A. G. Yodh[1]



Effects of Particle Shape on Growth Dynamics at Edges of Evaporating Drops of Colloidal Suspensions

Peter J. Yunker,[1] Matthew A. Lohr,[1] Tim Still,[1,2] Alexei Borodin,[3] D. J. Durian,[1] and A. G. Yodh[1]

[1]*Department of Physics and Astronomy, University of Pennsylvania, Philadelphia, Pennsylvania 19104, USA*

[2]*Complex Assemblies of Soft Matter, CNRS-Rhodia-University of Pennsylvania, UMI 3254, Bristol, Pennsylvania 19007, USA*

[3]*Department of Mathematics, Massachusetts Institute of Technology, Cambridge, Massachusetts 02139, USA*

(Received 23 July 2012; published 18 January 2013)

Effects of Particle Shape on Growth Dynamics at Edges of Evaporating Drops of Colloidal Suspensions

Peter J. Yunker,[1] Matthew A. Lohr,[1] Tim Still,[1,2] Alexei Borodin,[3] D. J. Durian,[1] and A. G. Yodh[1]

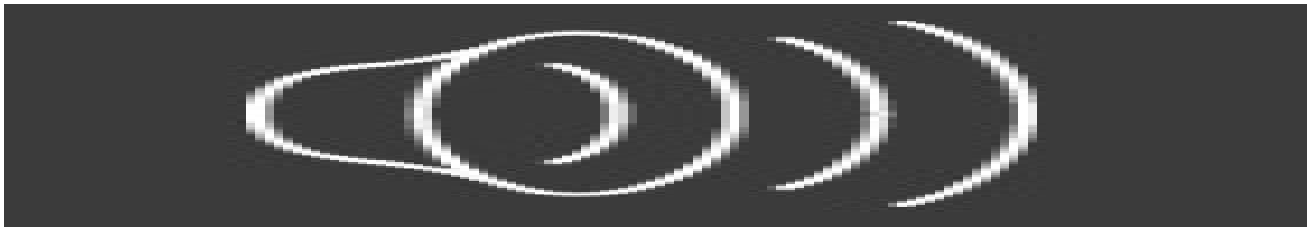
[1]*Department of Physics and Astronomy, University of Pennsylvania, Philadelphia, Pennsylvania 19104, USA*

[2]*Complex Assemblies of Soft Matter, CNRS-Rhodia-University of Pennsylvania, UMI 3254, Bristol, Pennsylvania 19007, USA*

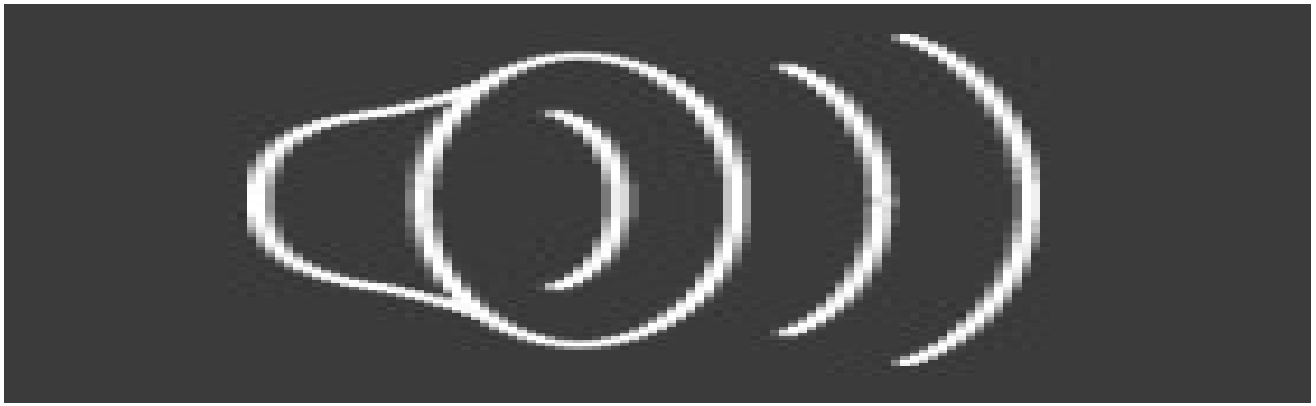
[3]*Department of Mathematics, Massachusetts Institute of Technology, Cambridge, Massachusetts 02139, USA*

(Received 23 July 2012; published 18 January 2013)

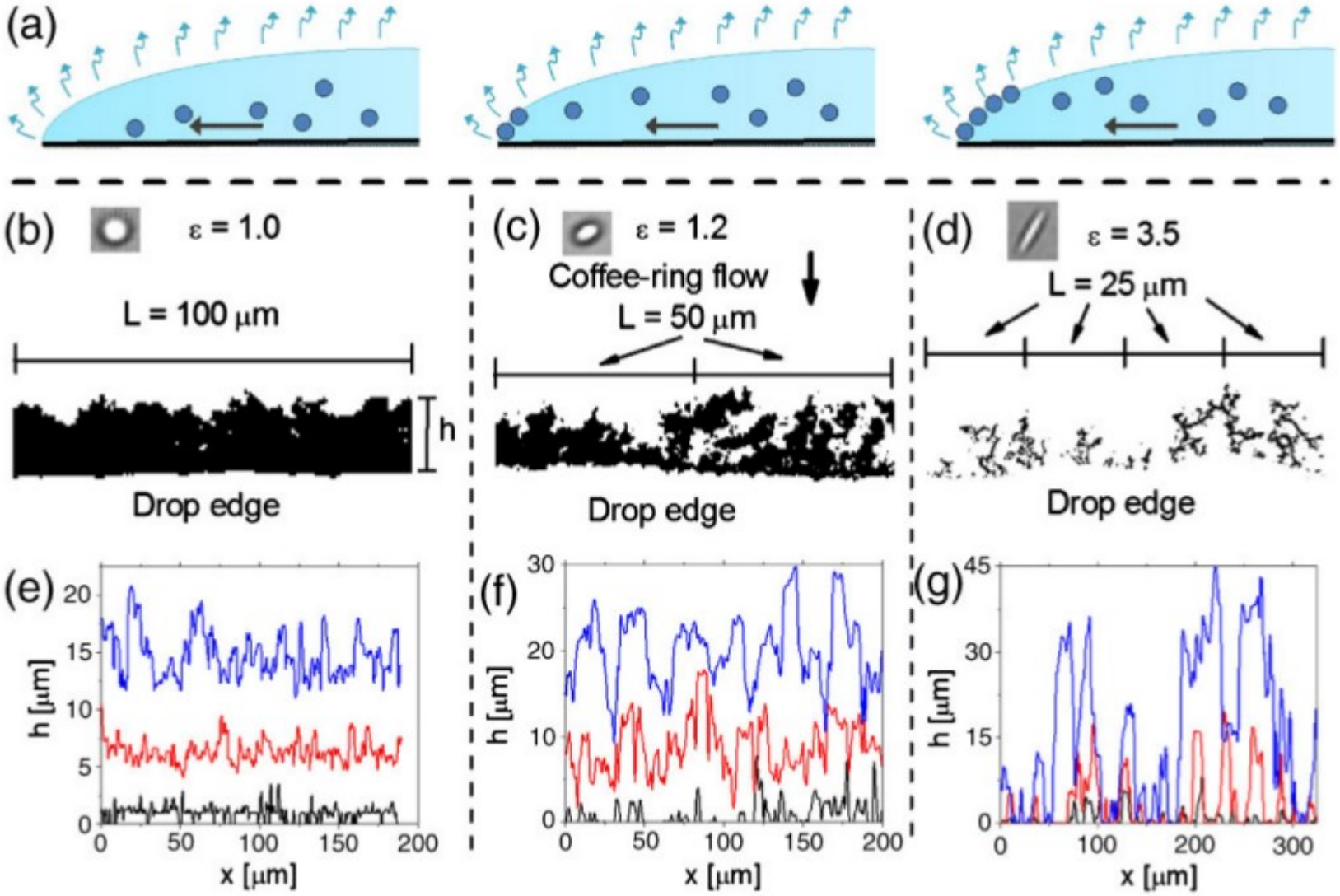
Particulas Esfericas



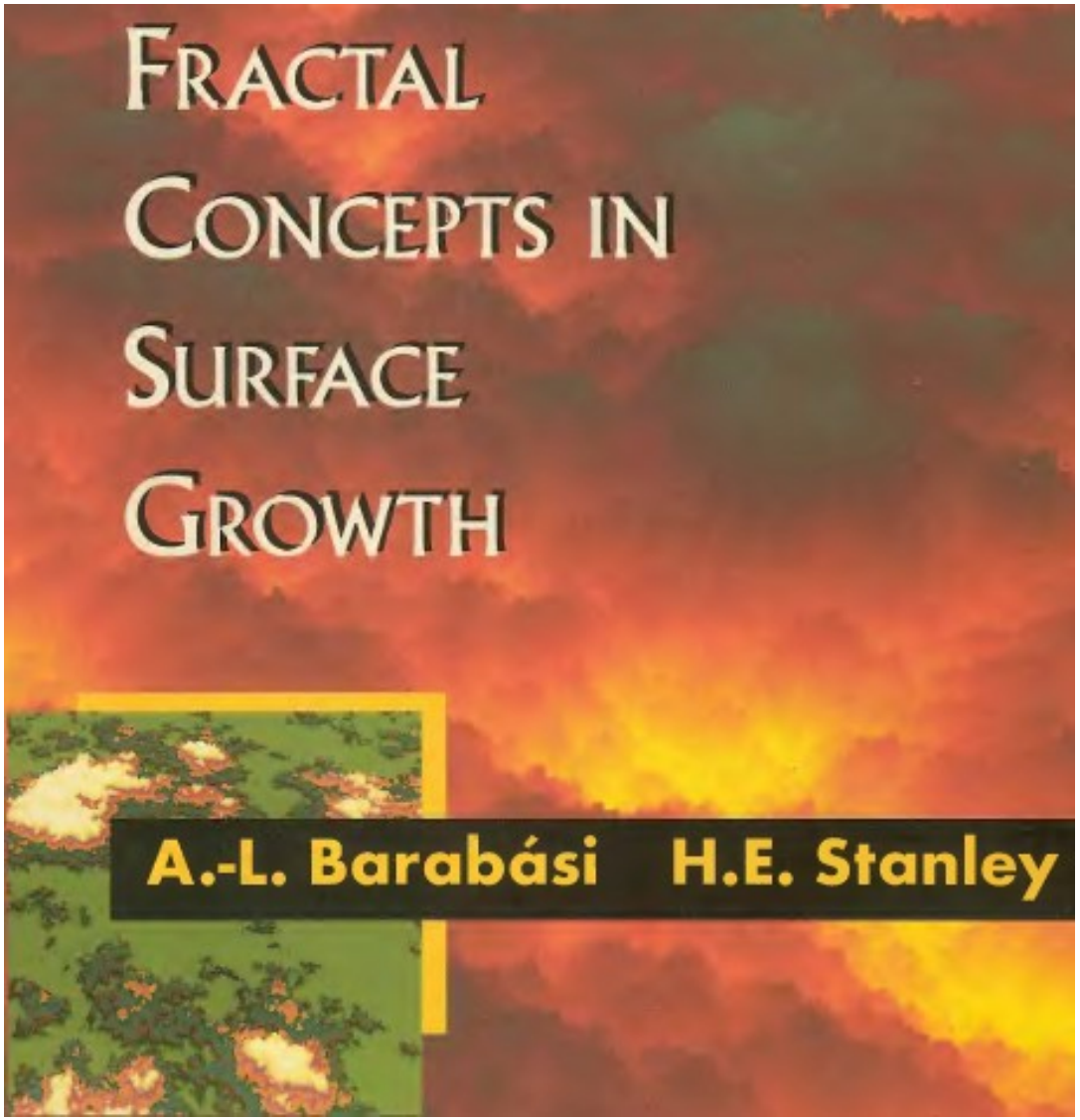
Particulas Oblongas



Deposición de partículas



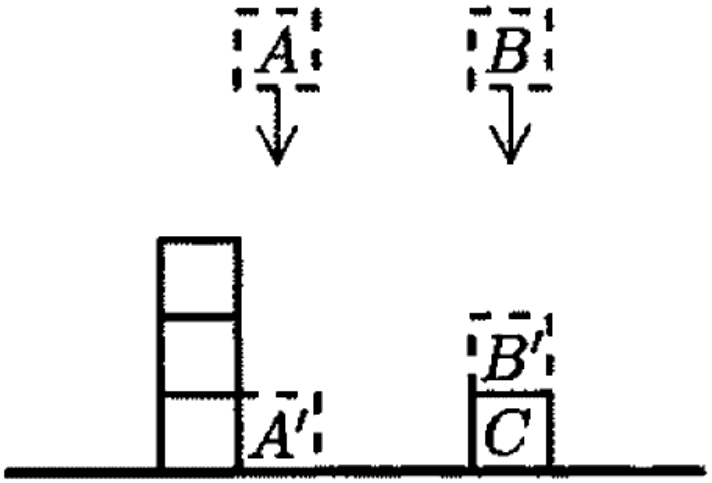
Clases de universalidad en el crecimiento de superficies



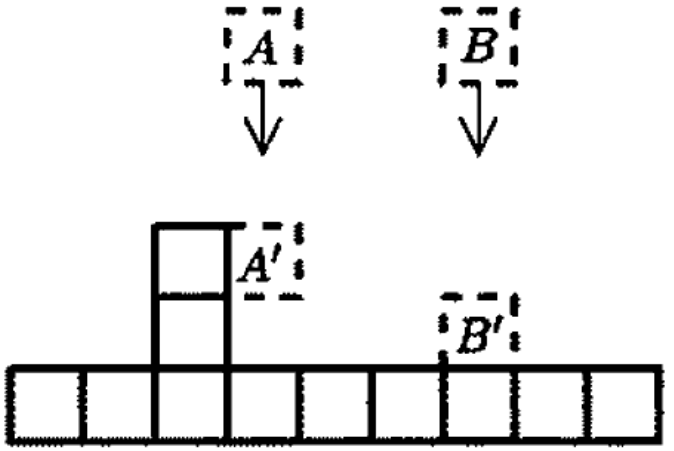
Clases de universalidad en el crecimiento de superficies

Modelos discretos simples (Tetris):

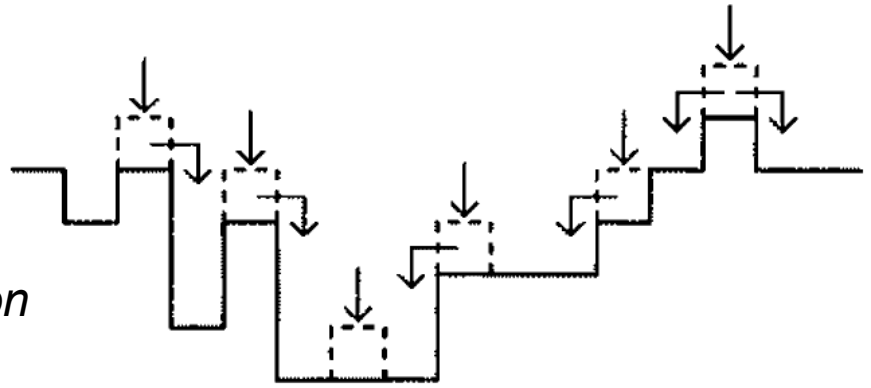
Random deposition



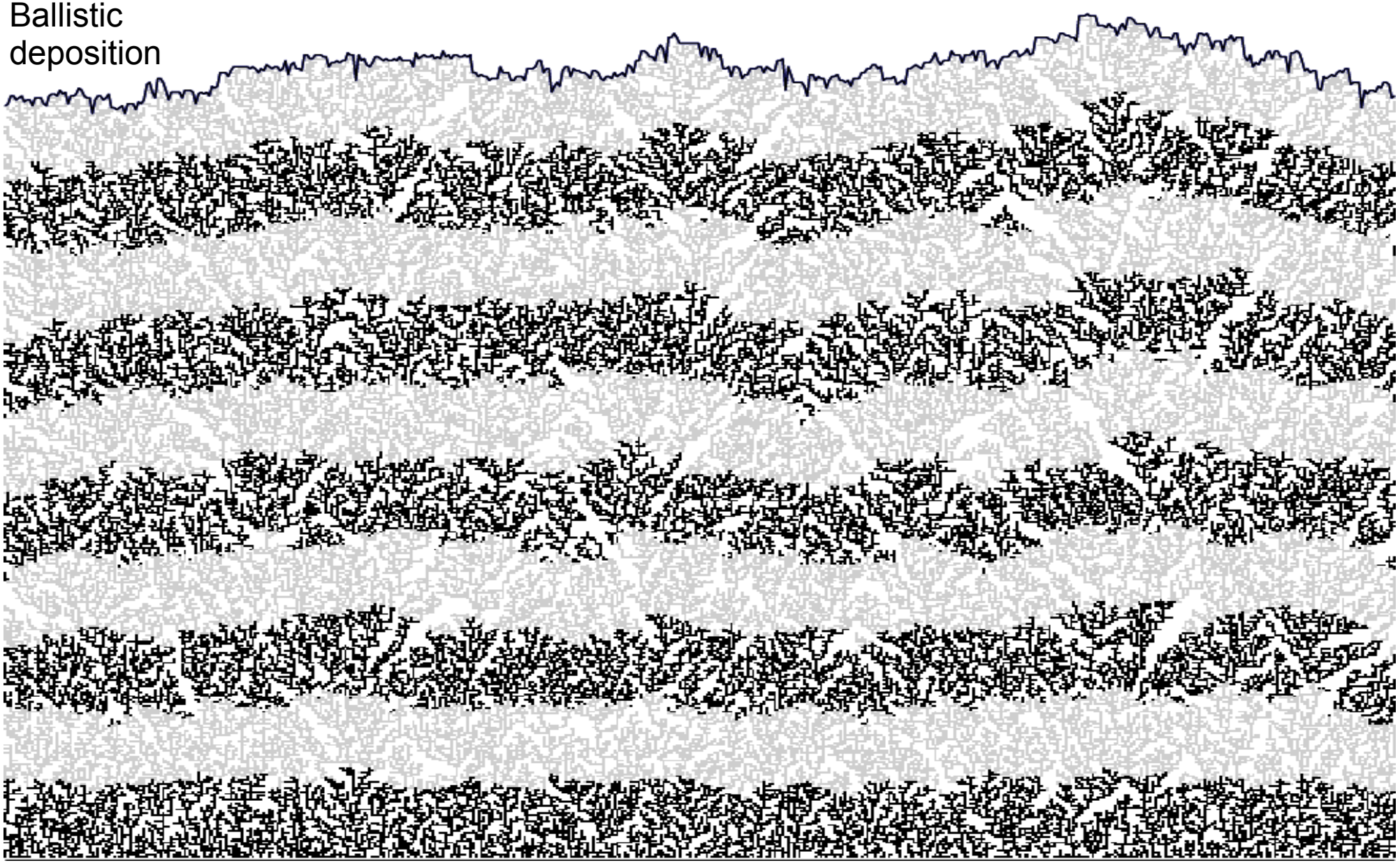
Ballistic deposition



Random deposition
With surface relaxation



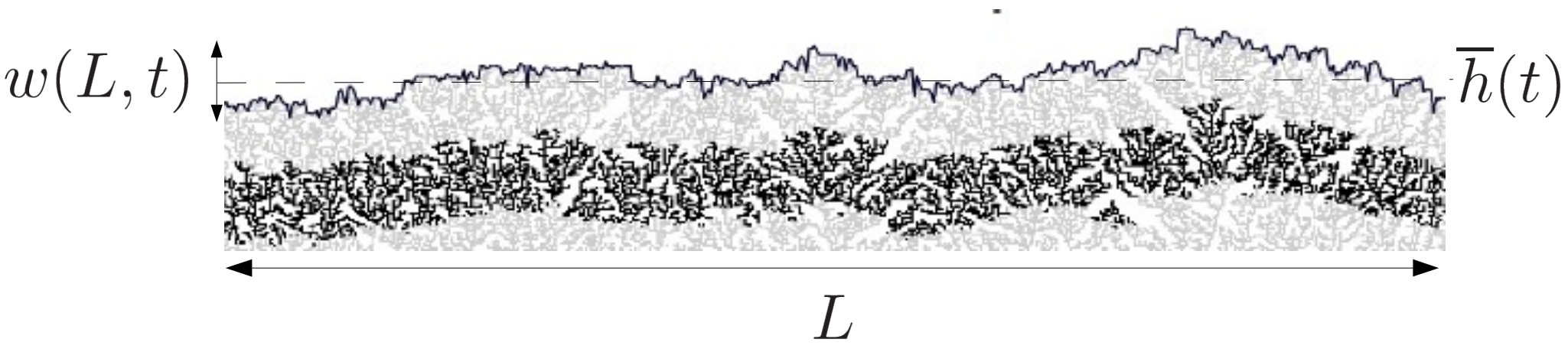
Clases de universalidad en el crecimiento de superficies



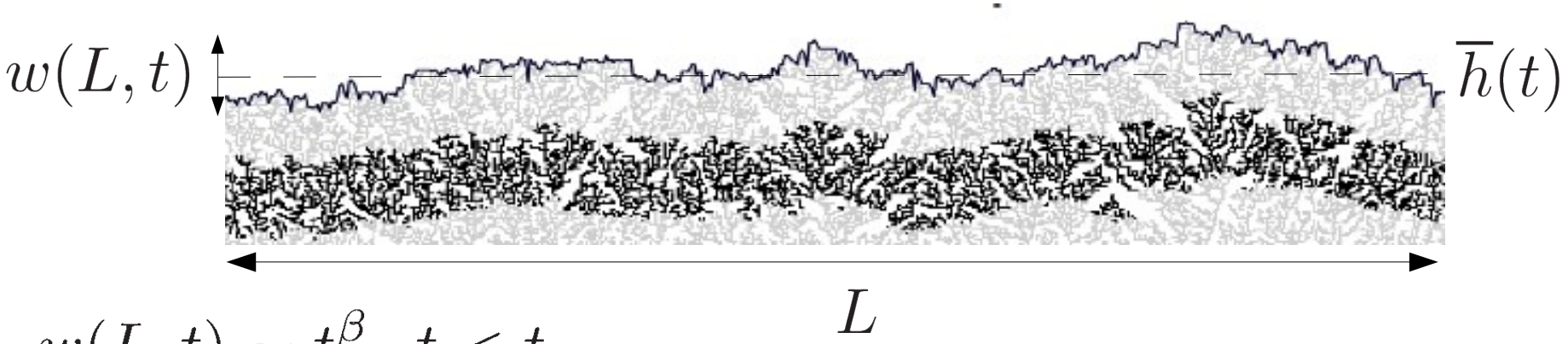
Clases de universalidad en el crecimiento de superficies

$$\overline{h}(t) = \frac{1}{L}\sum_{i=1}^{L} h(i,t)$$

$$w(L,t) = \sqrt{\frac{1}{L}\sum [h(i,t) - \overline{h}(t)]^2}$$

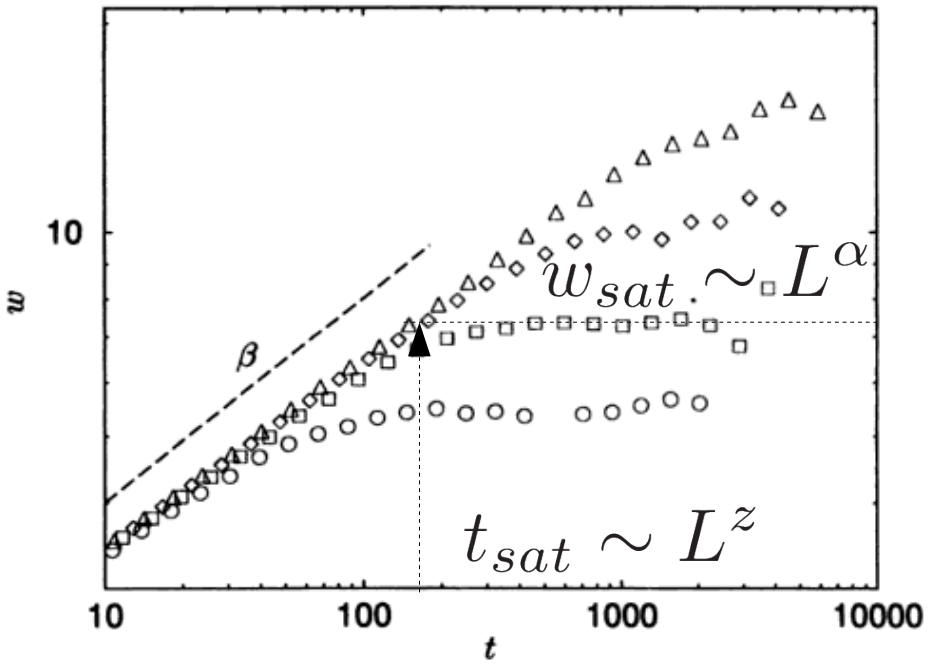


Clases de universalidad

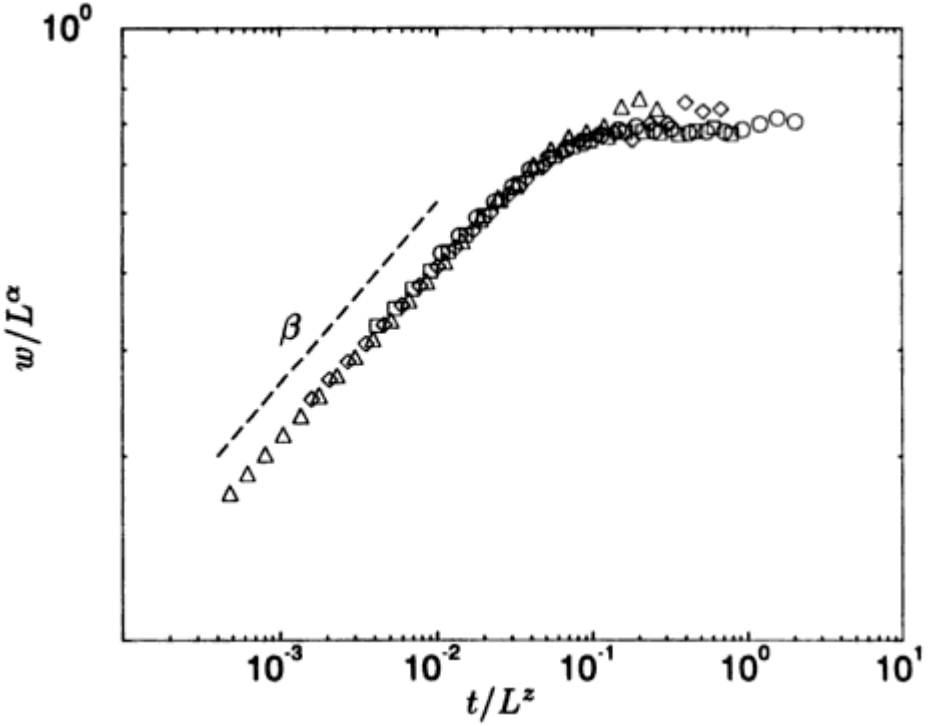


$$w(L,t) \sim t^{\beta},\ t < t_{sat}$$

$$w_{sat} \sim L^{\alpha},\ t > t_{sat}$$



$$w(L,t) \sim L^{\alpha} f(t/L^{z})$$



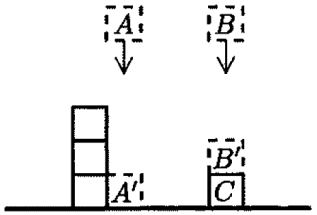
Scaling dinámico, Exponentes universales: $z,\ \beta,\ \alpha$

Tres clases importantes

- Modelos continuos (límite hidrodinámico RG)

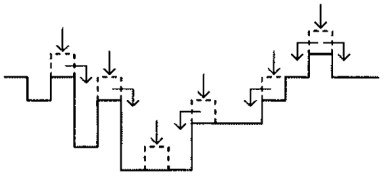
$$\langle \eta \rangle = 0,\ \langle \eta(x,t)\eta(x',t') \rangle = 2D\delta(t-t')\delta(x-x')$$

$$\partial_t h(x,t) = F + \eta(x,t)$$
$$\beta = 1/2 \rightarrow w(t) \sim [\overline{h}]^{1/2}$$



RANDOM DEPOSITION

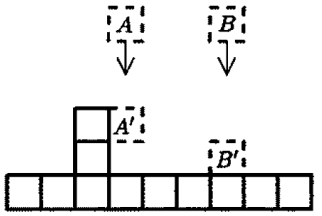
$$\partial_t h(x,t) = F + c\nabla^2 h(x,t) + \eta(x,t)$$
$$\alpha = (2-d)/2,\ \beta = (2-d)/4,\ z = 2$$



EDWARDS-WILKINSON

No-lineal!

$$\partial_t h(x,t) = F + c\nabla^2 h(x,t) + \lambda[\nabla h(x,t)]^2 + \eta(x,t)$$
$$\alpha = 1/2,\ \beta = 1/3,\ z = 3/2 \quad (d=1)$$



KARDAR-PARISI-ZHANG

Effects of Particle Shape on Growth Dynamics at Edges of Evaporating Drops of Colloidal Suspensions

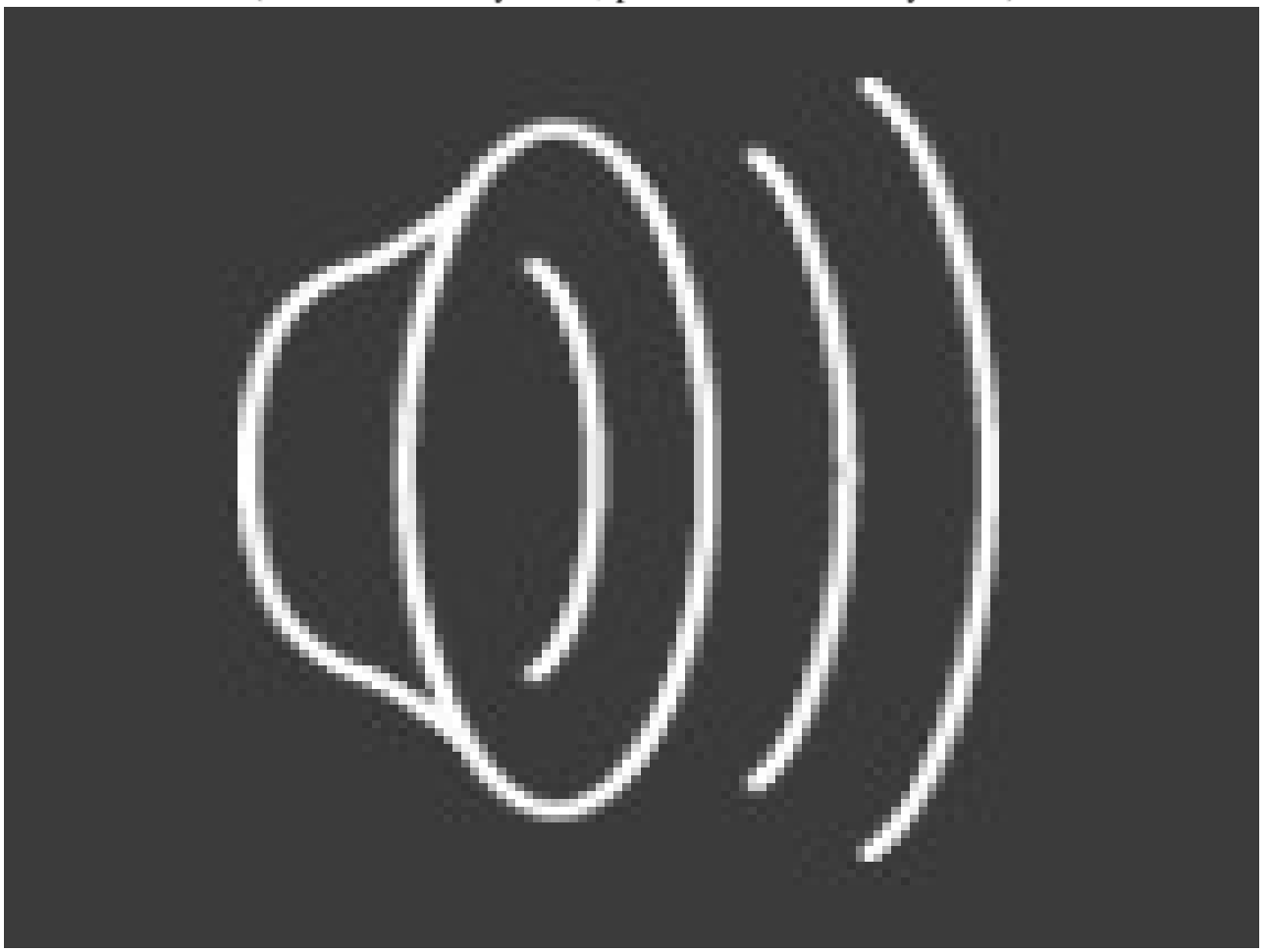
Peter J. Yunker,[1] Matthew A. Lohr,[1] Tim Still,[1,2] Alexei Borodin,[3] D. J. Durian,[1] and A. G. Yodh[1]

[1]*Department of Physics and Astronomy, University of Pennsylvania, Philadelphia, Pennsylvania 19104, USA*

[2]*Complex Assemblies of Soft Matter, CNRS-Rhodia-University of Pennsylvania, UMI 3254, Bristol, Pennsylvania 19007, USA*

[3]*Department of Mathematics, Massachusetts Institute of Technology, Cambridge, Massachusetts 02139, USA*

(Received 23 July 2012; published 18 January 2013)



Effects of Particle Shape on Growth Dynamics at Edges of Evaporating Drops of Colloidal Suspensions

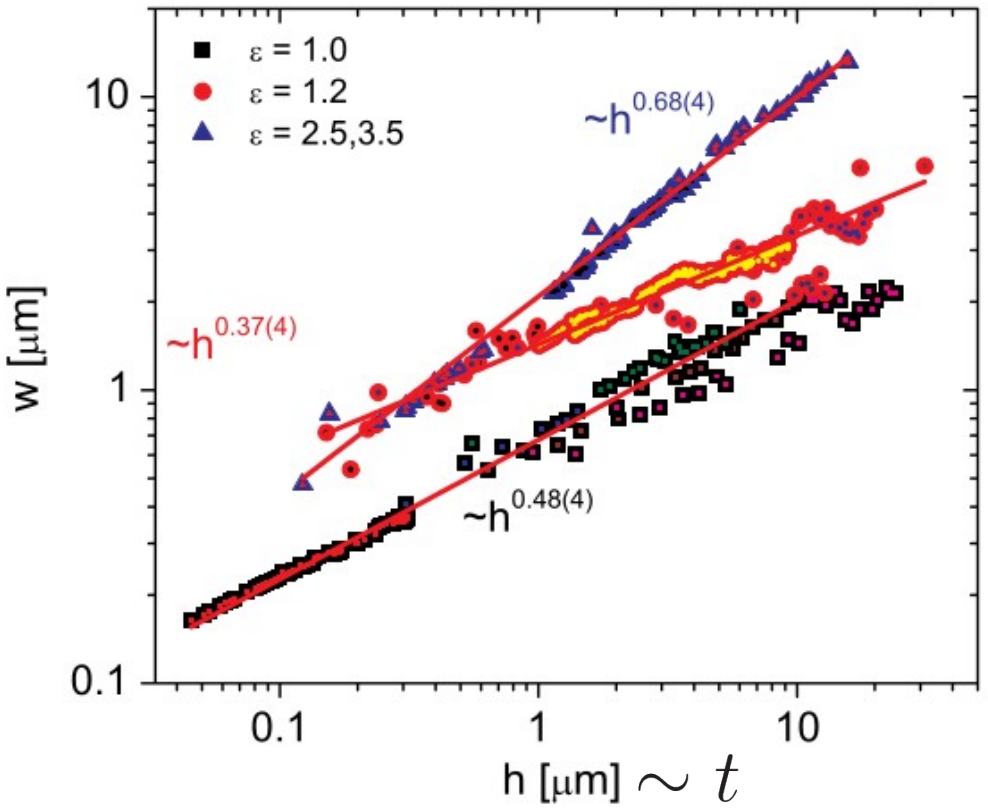
Peter J. Yunker,[1] Matthew A. Lohr,[1] Tim Still,[1,2] Alexei Borodin,[3] D. J. Durian,[1] and A. G. Yodh[1]

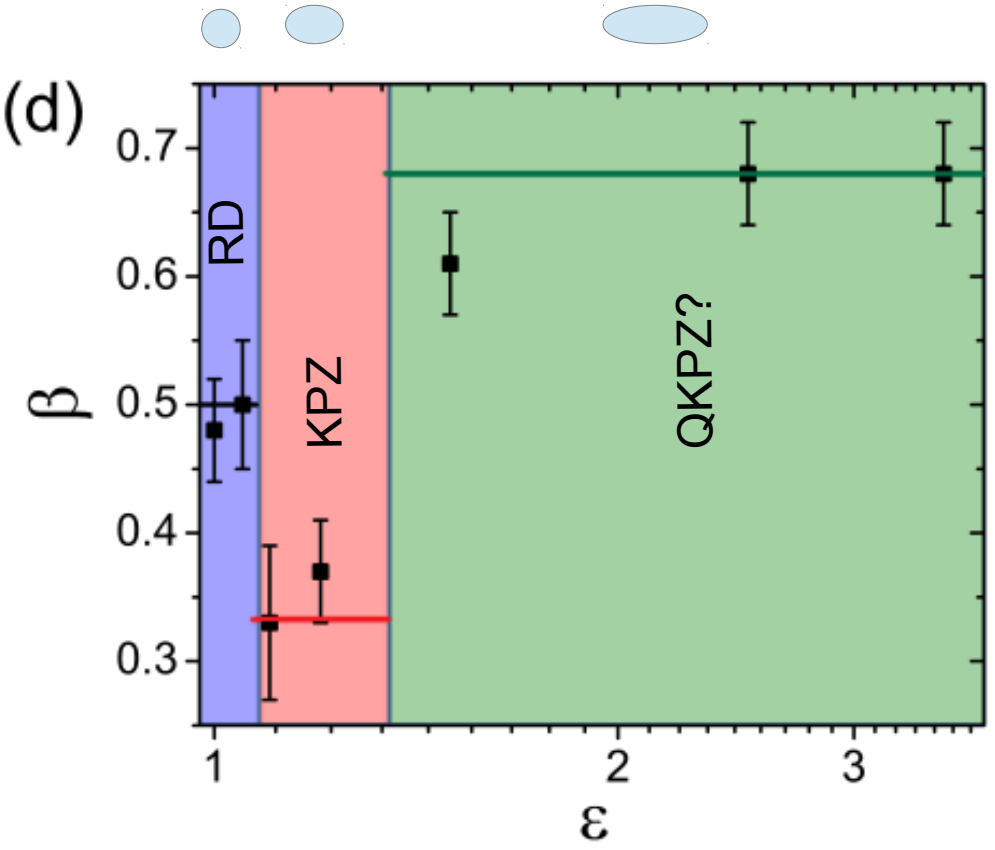
[1]*Department of Physics and Astronomy, University of Pennsylvania, Philadelphia, Pennsylvania 19104, USA*

[2]*Complex Assemblies of Soft Matter, CNRS-Rhodia-University of Pennsylvania, UMI 3254, Bristol, Pennsylvania 19007, USA*

[3]*Department of Mathematics, Massachusetts Institute of Technology, Cambridge, Massachusetts 02139, USA*

(Received 23 July 2012; published 18 January 2013)





Effects of Particle Shape on Growth Dynamics at Edges of Evaporating Drops of Colloidal Suspensions

Peter J. Yunker,[1] Matthew A. Lohr,[1] Tim Still,[1,2] Alexei Borodin,[3] D. J. Durian,[1] and A. G. Yodh[1]

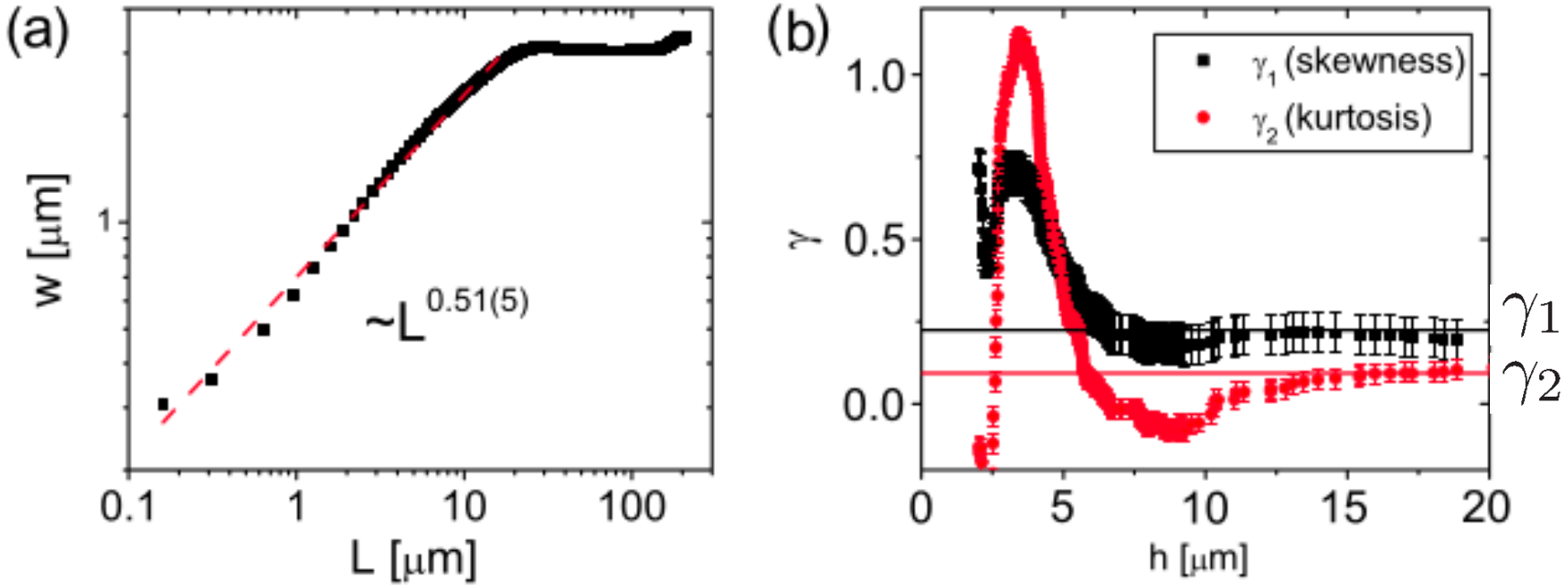
[1]*Department of Physics and Astronomy, University of Pennsylvania, Philadelphia, Pennsylvania 19104, USA*

[2]*Complex Assemblies of Soft Matter, CNRS-Rhodia-University of Pennsylvania, UMI 3254, Bristol, Pennsylvania 19007, USA*

[3]*Department of Mathematics, Massachusetts Institute of Technology, Cambridge, Massachusetts 02139, USA*

(Received 23 July 2012; published 18 January 2013)

$$\alpha_{KPZ} = 1/2 \qquad \gamma_{1,2}^{KPZ} = 0.22, 0.09$$



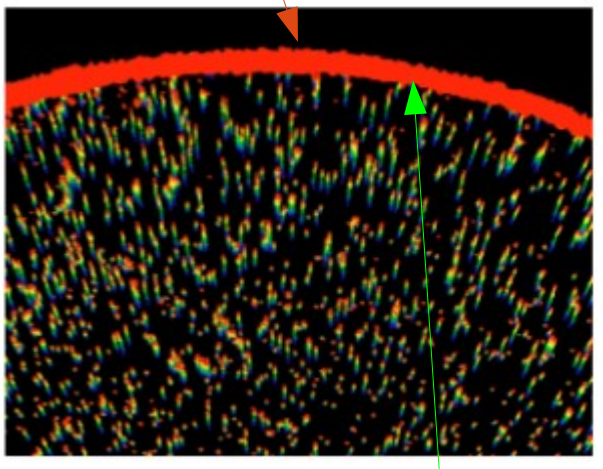
Tracy-Widom GUE ensemble

Interfases everywhere!

Linea de triple contacto:

$$\frac{\partial}{\partial t}h(x,t) = f + \eta(x,h) - k\int dx_1 \frac{h(x,t) - h(x_1,t)}{(x-x_1)^2} \, .$$

Ruido "congelado"



Frente de deposición:

$$\partial_t h(x,t) = F + c\nabla^2 h(x,t) + \lambda[\nabla h(x,t)]^2 + \eta(x,t)$$

Ruido "térmico"

Inkjet-Printed Line Morphologies and Temperature Control of the Coffee Ring Effect

Dan Soltman* and Vivek Subramanian

Department of Electrical Engineering and Computer Science, University of California, Berkeley, California 94720

Received August 30, 2007. In Final Form: October 17, 2007

We have studied inkjet-printed drops of a conductive polymer. We show how varying drop spacing and temperature lead to several different printed line morphologies and offer a simple geometric explanation for these various forms. Also, by controlling the evaporation profile of drying drops and lines, we demonstrate control of the coffee ring effect by which solute is transferred to the rim. Under appropriate conditions, we are able to enhance or eliminate the coffee ring effect in our drying features.

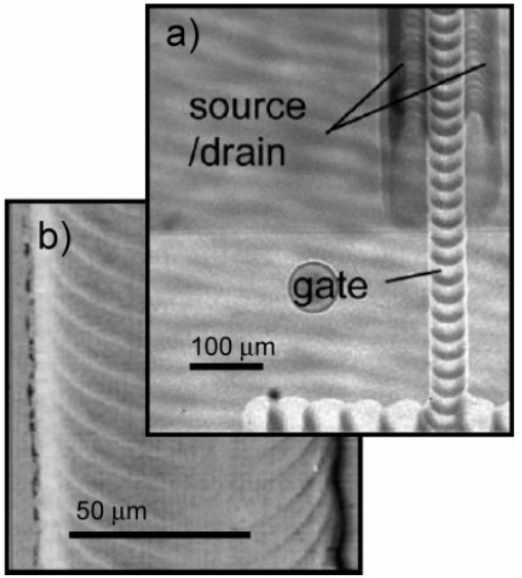


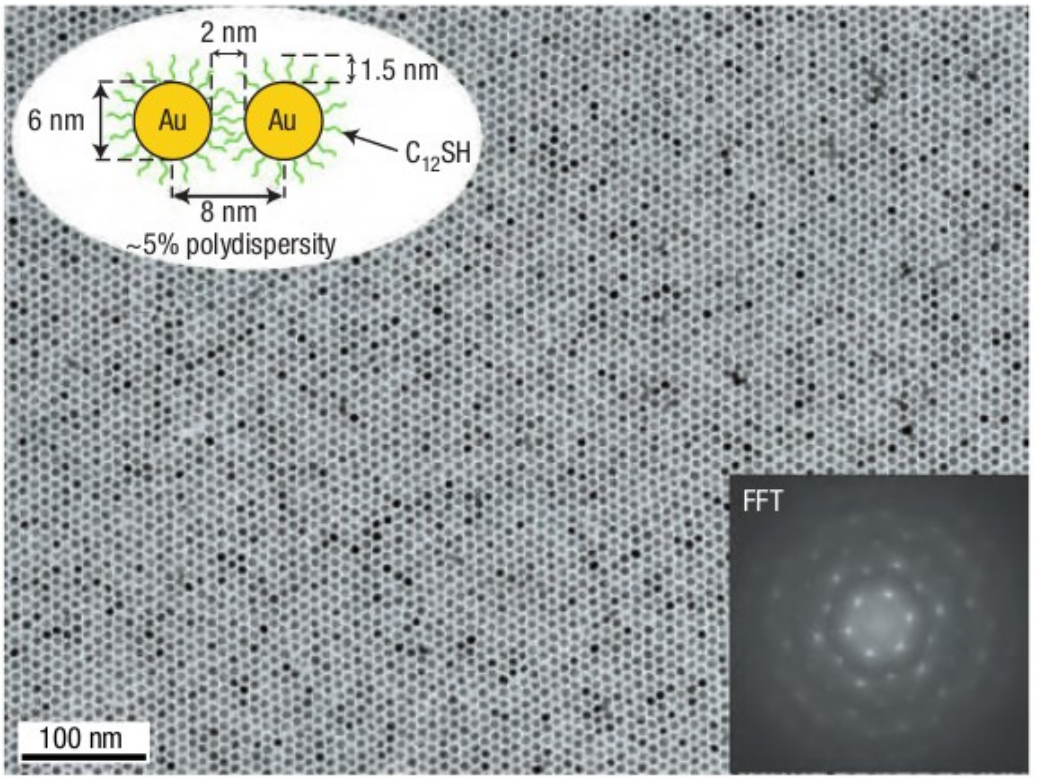
Figure 1. (a) Micrograph of inkjet-printed TFT with pedot contacts[4] and (b) AFM of an inkjet-printed gold nanoparticle line.[2]

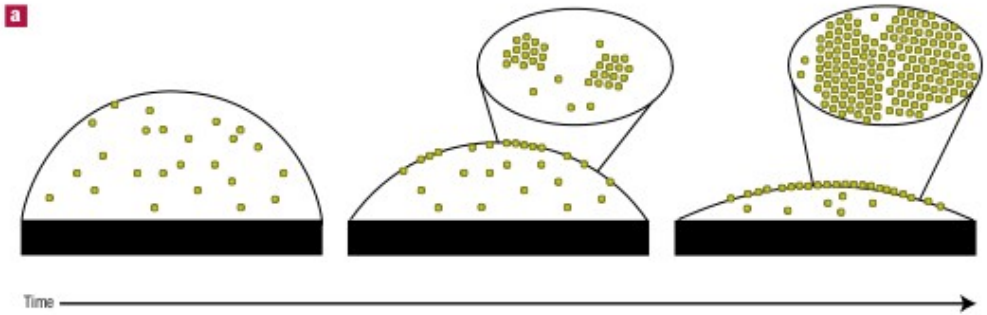
Kinetically driven self assembly of highly ordered nanoparticle monolayers

nature materials | VOL 5 | APRIL 2006 |

TERRY P. BIGIONI[1], XIAO-MIN LIN[2], TOAN T. NGUYEN[1], ERIC I. CORWIN[1,3], THOMAS A. WITTEN[1,3] AND HEINRICH M. JAEGER[1,3]*

[1]James Franck Institute, University of Chicago, Chicago, Illinois 60637, USA
[2]Materials Science Division, Chemistry Division and Center for Nanoscale Materials, Argonne National Laboratory, Argonne, Illinois 60439, USA
[3]Department of Physics, University of Chicago, Chicago, Illinois 60637, USA
*e-mail: h-jaeger@uchicago.edu



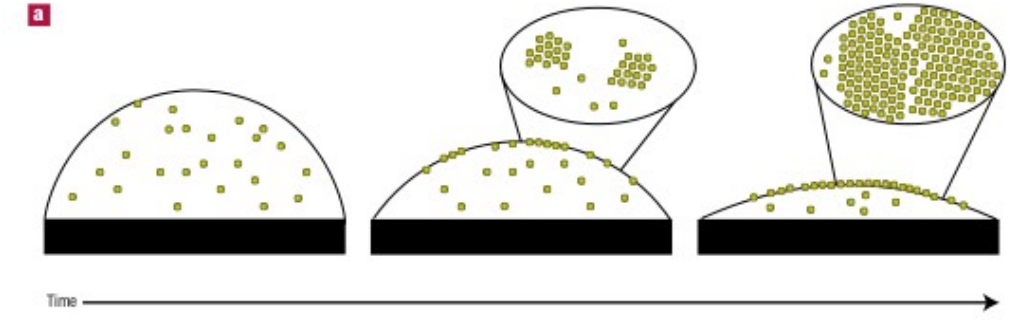


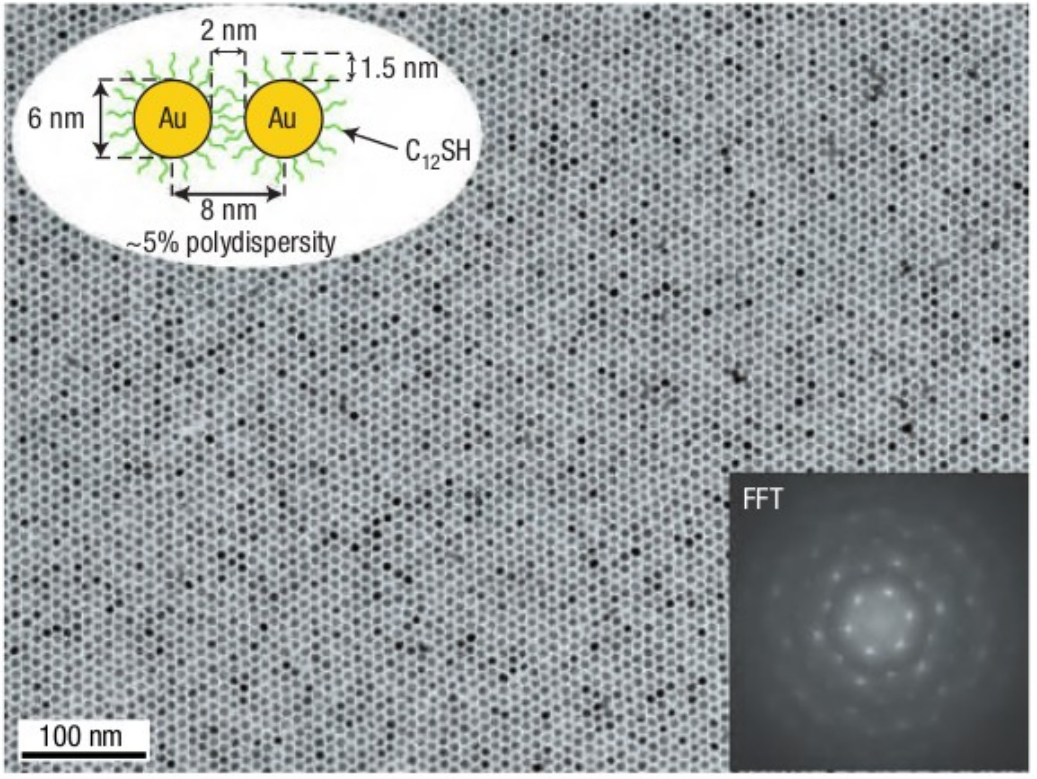
Kinetically driven self assembly of highly ordered nanoparticle monolayers

nature materials | VOL 5 | APRIL 2006 |

TERRY P. BIGIONI[1], XIAO-MIN LIN[2], TOAN T. NGUYEN[1], ERIC I. CORWIN[1,3], THOMAS A. WITTEN[1,3] AND HEINRICH M. JAEGER[1,3]*

[1] James Franck Institute, University of Chicago, Chicago, Illinois 60637, USA
[2] Materials Science Division, Chemistry Division and Center for Nanoscale Materials, Argonne National Laboratory, Argonne, Illinois 60439, USA
[3] Department of Physics, University of Chicago, Chicago, Illinois 60637, USA





191- ANALES AFA Vol. 11 TUCUMAN 1999 - 191

ORDEN Y DIAGRAMA DE FASES EN SISTEMAS BINARIOS BIDIMENSIONALES

P. S. Cornaglia*, A. B. Kolton, D. Domínguez
Instituto Balseiro, Centro Atómico Bariloche
Universidad Nacional de Cuyo
(8400)S. C. de Bariloche, Río Negro, Argentina.
*cornagli@cab.cnea.gov.ar

Presentamos simulaciones de dinámica de Langevin de un sistema bidimensional binario de partículas de Lennard-Jones. Estudiamos el orden traslacional, orientacional y topológico de la red y la difusión en función de la dispersividad (diferencia de tamaño entre las partículas) y la temperatura. En base a los resultados obtenidos confeccionamos un diagrama de fases. Las distintas estructuras encontradas se corresponden con las observadas por otros autores en experimentos con sistemas binarios de nanopartículas de oro.